

AN ABSTRACT OF THE THESIS OF

Nicholas Steven Jude Aerne for the degree of Master of Science in Mechanical Engineering presented on February 27, 2018.

Title: Adhesive Properties Subject to Variation in Temperature, Thickness, and Working Time

Abstract approved:

John P. Parmigiani

Adhesive use is becoming increasingly common in manufacturing processes. The advantage of adhesives are light weight components, non-destructive fastening techniques and distribution of loads over the applied bond region. Modeling the behavior of adhesive bond lines in fastening joints can help in the design process to make an optimized joint, with minimal adhesive waste. However, the material properties provided by manufactures of adhesives often creates a gap in what is sufficient to accurately model the behavior of real-world adhesive conditions. To design optimized joints, the loading conditions, environmental conditions of service, thickness of bond, and bonding procedures all need to be refined for the adhesive of interest. The body of research presented for this thesis are the results of two phases of adhesive testing to meet these conditions for optimized adhesive joints. In Phase I, the temperature is varied and tested against two adhesives, Plexus MA832 and Pliogrip 7779/220b, and four specimen types. The specimens serve the purpose of providing the needed material properties to compose a traction separation law (TSL) in loading

mode I and mode II. The needed material properties to compose an accurate TSL have been shown to be the mode I cohesive strength, mode I cohesive toughness, mode II cohesive strength, and mode II cohesive toughness. These properties can be measured with test specimens designed to isolate the specific loading mode and condition. The specimens used are the Dog Bone Tensile Specimen, the Double Cantilever Beam (DCB), Shear Loaded Dual Cantilever Beam (SLDCB), and Double Lap Shear. In Phase II the thickness, working time, and temperature are varied for Plexus MA832 with the DCB and SLDCB specimens. The adverse condition that the environmental temperature changes have on adhesive property behavior will be simulated with a temperature chamber. The chamber was used to test specimens at -30°C, -20°C, 20°C, 40°C and 45°C. The thickness varied in Phase II was 1.27 ± 0.34 [mm] for a thin bond and 10.38 ± 0.66 [mm] for a thick bond. The working time varied in Phase II had a control group bonded in the recommended working time for all thicknesses, and an expired working time where the specimens were not joined until 10 [min] had passed from the recommended working time. Triplicates of each specimen at the respective conditions were tested for both phase I and II. The use of adhesives in adverse temperature conditions is advised to be tested and refined in design before implementation into service. The findings of this report have shown that adhesive factors such as temperature conditions, thickness of bond, and working time can be found to have degraded performance on adhesive load carrying ability in mode I and mode II.

©Copyright by Nicholas Steven Jude Aerne
February 27, 2018
All Rights Reserved

Adhesive Properties Subject to Variation in Temperature, Thickness, and Working
Time

by
Nicholas Steven Jude Arne

A THESIS

submitted to

Oregon State University

in partial fulfillment of
the requirements for the
degree of

Master of Science

Presented February 27, 2018
Commencement June 2018

Master of Science thesis of Nicholas Steven Jude Aerne presented on February 27, 2018

APPROVED:

Major Professor, representing Mechanical Engineering

Head of the School of Mechanical, Industrial, and Manufacturing Engineering

Dean of the Graduate School

I understand that my thesis will become part of the permanent collection of Oregon State University libraries. My signature below authorizes release of my thesis to any reader upon request.

Nicholas Steven Jude Aerne, Author

ACKNOWLEDGEMENTS

The author expresses sincere appreciation for the support and guidance of Major Advisor Dr. John Parmigiani during the pursuit of this Masters. The advice he has provided has enabled success and growth in not only the field of Mechanical Engineering, but in situations found outside of laboratory basements.

The graduate students in Covell 001 have been a pleasure to study alongside, it is my wish to express gratitude to them here, in order of appearance, Mark McGuire, Levi Suryan, Mitch Daniels, Rajib Mahabub, Taylor Rawlings, Eric Shannon, Alexander Orawiec, and many others from and outside the computational mechanics and applied design laboratory.

Taylor Rawlings aided the manufacturing, cleaning, abrading, and gluing of the test specimens. His assistant decreased the overall preparation time of the specimens greatly, increasing the pace of progress towards this degree. Additional thanks is expressed here.

The opportunity to be involved with the MRPL shop faculty as a graduate teaching assistant has been a unique pleasure that I would not trade for all the nearby Allen wrenches. The support of the shop provided the ability for growth in my engineering communication skills and allowed the continuation for progress towards this degree. I have found, and will continue to find, great appreciation for this opportunity. To those of the shop, thanks.

Additionally, I would like to thank Daphne Mattos, and Sophie for all of the coffee and support,

And lastly, my parents, family, and friends of which would be superfluous to name here. For without all of the above, none of the below would exist.

TABLE OF CONTENTS

Page

- 1. Introduction 1
- 2. Literature Review 9
 - 2.1 Adhesives Origin..... 9
 - 2.2 Fracture Mechanics10
 - 2.3 Cohesive Zone Modeling14
 - 2.4 Adhesive Parameters19
- 3. Materials and Methods 21
 - 3.1 Test Ready Specimens.....21
 - 3.2 Manufacturing and Testing Steps25
 - 3.3 Pliogrip Prep.....30
- 4. Results 43
 - 4.1 Phase I -48
 - 4.2 Tabled Results – Phase I and Phase II.....60
- 5. Discussion..... 66
- 6. Conclusion..... 70
- Future Work and Recommendations 72
- Bibliography 73
- Appendix..... 78
 - A bill of materials.....78
 - Raw Stock79
 - Sheet drawings of specimens.....80

LIST OF FIGURES

<u>Figure</u>	<u>Page</u>
Figure 1- Traction separation law on a mode I tension specimen	15
Figure 2 – DBTS test specimen ready for testing	22
Figure 3 – DCB specimen ready for testing.....	23
Figure 4 – DLS specimen ready for testing	23
Figure 5 – SLDCB specimen ready for testing	24
Figure 6 – DCB and SLDCB CNC fixture	28
Figure 7 – DBTS CNC fixture	28
Figure 8 – DLS specimen fixture.....	29
Figure 9 – Pliogrip specimens with layer of SMC.....	30
Figure 10 – DCB, SLDCB bond line fixture on an SLDCB specimen.....	34
Figure 11 – DBTS bond line fixture	34
Figure 12 – Thermocouple placement on DCB, DBTS, and SLDCB specimens.....	36
Figure 13 – Steel loading extenders for the loading fixtures.....	37
Figure 14 – DCB and DBTS loading fixtures.....	38
Figure 15 – left- Self-tightening grips for testing DLS specimens in the temperature chamber at -30°C in the Instron testing machine.....	39
Figure 16 – right - Shear loading fixture for testing the SLDCB specimen in the Instron testing machine	39
Figure 17 – Temperature chamber built by Meraz at Oregon State University.....	41

LIST OF FIGURES (Continued)

<u>Figure</u>	<u>Page</u>
Figure 18 – DBTS specimen results	44
Figure 19 – DCB specimen results	45
Figure 20 – DLS specimen results	46
Figure 21 – SLDCB specimen results.....	47
Figure 22 – DBTS specimen results	48
Figure 23 – DCB specimen results	49
Figure 24 – DLS specimen results	50
Figure 25 – SLDCB specimen results.....	51
Figure 26 – DCB specimen results	52
Figure 27 – DCB specimen results	53
Figure 28 – DCB specimen results	54
Figure 29 – DCB specimen results	55
Figure 30 – SLDCB specimen results.....	56
Figure 31 – SLDCB specimen results.....	57
Figure 32 – SLDCB specimen results.....	58
Figure 33 – SLDCB specimen results.....	59
Figure 34 – Adhesive Failure type: Left-Cohesive, Middle-Adhesive, Right-Substrate	67

LIST OF TABLES

<u>Table</u>	<u>Page</u>
Table 1 - Results for Plexus MA832.....	61
Table 2 - Results for Pliogrip 7779/220.....	62
Table 3 - Results for Plexus MA832 variation in thickness, working time and temperature	63
Table 4 – Summary of Statistical Differences Phase I	64
Table 5 – Summary of Statistical Differences Phase II	65

1. Introduction

Often in design, there is a need to join two materials together. The materials chosen to be fastened together have a few options; the materials could be welded together as long as their microstructures can be fused with heat, a thru hole could be placed in each material and either a bolt, press fit pin or rivet applied, the materials may have interlocking geometry that use friction to hold them together, or the materials may be joined with adhesives. The first of these options requires the materials to be compatible with each other, and requires additional work to heat the materials together. Any fastening method that involves placing a hole for a bolt, or similar application, requires destructive actions on the materials to be able to manufacture the hole. This manufacturing will also induce a stress concentration at the hole location. There will also be mass added to the system due to the bolt assembly. The ability to use interlocking geometry requires complex geometry, implementation planning, and intricate assembly, which adds considerable time during the design process. The remaining listed fastening method is to adhere the two work pieces together with adhesives.

The process of adhesion provides a few benefits to the fastening process over the other methods presented. Namely adhesion does not require; additional heating to fuse the materials together, the process can be non-destructive to the substrates, the force the fastened materials experience through load is not concentrated at a location, but rather distributed over the bond region, the adhesive is able to join dissimilar materials and in most cases, there is a reduction in the weight of the component.

Though adhesives have these benefits, to successfully design adhered components to efficiently utilize the properties of adhesives can often be a challenging task.

The modeling of adhesive bond lines in joint design is an increasing demand across industry. The motivation in industry stems from the reasons listed previously. In order to model adhesive bond lines properly in Finite Element Analysis (FEA), accurate adhesive behaviors and properties are needed. Without accurate adhesive behaviors, to obtain a proper adhesive bond for a given joint, a trial and error style approach is required. This approach can be time consuming and wasteful in the design phase to get an adhesive bond to support its load requirements, and be utilized efficiently, that is to not be severely over-designed, and have minimal material waste.

The material properties of an adhesive needed for sufficient modeling behavior can be measured from test specimens. The test specimens to provide adhesive properties embody loading types and conditions that are relevant to the joint behavior under load. There are three loading types. Loading type one, called mode I loading, is an opening or tensile load. Loading type two, called mode II loading, is a sliding or in-plane shear load. Lastly, loading type three, called mode III, is a tearing or out-of-plane load. The first two loading modes are sufficient to model the majority of loading scenarios a joint will see in service.

The loading condition within the loading type helps to define the behavior of the adhesive. There are two loading conditions of interest, the strength and toughness. The strength of a material is the ability of the structure to resist permanent deformation. For example, in metal crystal structures when a force is applied to the material, and the structure has absorbed enough load to move a dislocation. This

dislocation movement creates a damaged region where the stress concentration of the force was applied. This damaged region does not return to its initial unloaded-undeformed state. The strength of the metal in this example is the threshold for the structure to prevent this damage, from dislocation movement, from occurring.

The toughness of a material is the ability of the structure to resist complete failure after permanent deformation has occurred. For example, in a metal crystal structure once the structure has begun to yield, take on damage in the form of dislocation movement, the material will continue to be damaged until a point where a crack will form in the structure. The progression of damage until the occurrence of a crack in the yielded or permanently deformed material is the toughness of the metal crystal structure. Another way to think about the toughness of a structure is a materials ability to absorb energy, from permanent deformation until failure. The max energy release rate, which is an aspect of the toughness. Is defined as the amount of energy per unit volume that a material can absorb before crack growth. The energy release rate is useful for relating the toughness of adhesives.

Both the strength and toughness of an adhesive are needed to yield an effective model. These two loading conditions combined with the previous two types of loads creates a detailed look into how the adhesive layer will behave under load until failure. Predicting when the adhesive will fail with modeling that uses these parameters will produce a better result than a comparison of a single parameter often presented by adhesive manufactures. These parameters will also give meaningful adhesive behavior data that trial and error style approaches miss.

The tradeoff here, is in trial and error style approaches a specific loading condition, and type of failure can be found. However, the specific loading condition and type cannot be easily identified or separated from this procedure. Therefore, changes made between each iteration do not access the behavior of the adhesive, but rather the reaction of the adhesive layer in the joint subjected to the tested loading condition, which remain unknown and may change when testing structures of unique geometry. The approximate loads a bonded joint will hold at any operating condition is currently best found by performing destructive testing methods, but the true adhesive behavior is not found with this approach.

It is found that available adhesive material property data sheets from manufactures often lack sufficient information on needed materials properties to be able to design an effective adhesive joint. The tests often administered to determine the properties of adhesives by adhesive manufactures are not always applicable to how the adhesive will be loaded in service, e.g., an adhesive manufacture may test and report the materials properties for a tensile loading condition under standard laboratory environments. Another issue in material property data sheets for adhesives is not reporting the adherent material the adhesive was bonding together during testing, if an adherent was even utilized. The geometry used in standards for adhesives can be drastically different from the final purposed application [1]. An example of this occurs in the peeling force of an adhesive versus the strength of the adhesive under a distributed tensile load. This can be easily visualized by considering a piece of tape on a flat surface. To remove the tape, it is much easier to peel the tape

away from the edge then to try to grip the entire area of the tape and remove it all at once.

Often, the effects of the environmental conditions that the adhesive is subjected to in service are not available, due to the majority of manufacture property data coming from a laboratory environment. The material properties that are found from manufactures usually provide a reference to decide if one adhesive has greater strength than the other does, but will not yield optimal design [2]. The selection of adhesives for adverse temperature conditions in service requires an adhesive test at the operating temperature range in advance to implementation [2]. This test would have to be performed after a prototype is being tested in adverse conditions, and without prior environmental testing of the adhesives, its performance would be unknown.

Some adhesive components are utilized by providing a gap filling application. A gap-filling adhesive is used to fill space between components. An example of this is when different materials are joined and welding cannot be used to fill the space. Another example is when the entire space is desired be filled but extending the materials is not possible. Gap filling applications may also create spaces where there are different thicknesses of adhesive. The properties of specific thicknesses are not often provided by manufactures. Usually manufactures provide an ideal gap thickness for adhesives, and little is given on behavior outside of this range.

In adhesives that cure to full strength there is usually an associated working time and cure time. The working time of the adhesive is the time when the adhesive can be worked and applied to the materials it is joining. The cure time is the time

needed by the adhesive to achieve full strength. Often a manufacturer will report conditions that the adhesive should be applied in, and a range for both the working time and the cure time. However once again there is little information about the adhesive behavior outside of these reported ranges.

Often the decision between manufacturer data sheets one is left with to make is whether the tensile strength of one adhesive is greater than the other. This relative comparison does not help joint design when environmental factors, adhesive conditions, or adherent surfaces are needed in the design process. Even if one manufacturer reports a full set of material properties, the insight of one adhesive's behavior is not an embodiment of every adhesive bond. A comparison between adhesives should, at a minimum, consider the adherent materials, the loading conditions, the environmental conditions, the thickness of the adhesive region, and the bonding procedure. As these factors have been known to effect adhesive performance [3, 4,5,6,7].

Daimler Trucks North America (DTNA), a local freight truck manufacturer, is interested in reducing testing and product waste costs by optimizing the adhesive joints in their products. DTNA has sponsored a three-year project to accomplish this task. To achieve joint optimization, accurate adhesive behaviors are needed. The behavior during a range of environmental conditions was desired. The trucks produced by DTNA are purchased in the USA, Canada, Mexico, and 35 other countries outside of North America [8]. The geographical conditions of these locations result in a wide range of temperatures the trucks are to provide

transportation services. DTNA identified the temperature as the environmental condition of interest for the present study.

DTNA uses adhesives in multiple applications within the trucks that they manufacture. One example of a place that adhesives are used to fasten together materials is to bond various components of the truck cabin. Another region of the truck that utilizes adhesives is the hood. A composite hood is used on several trucks by DTNA that is bonded to the frame of the vehicle by hood supports and brackets. The region between the underside of the hood and the hood supports on the frame retain the adhesive layer. The different application of adhesives on the freight trucks require various adhesives to yield a desired product.

The use of different adhesives is required to meet the requirements of the components in and on the freight truck. The components of the truck cabin for example will have different bond strength requirements, environmental conditions, base materials, bond toughness requirements, and adhesive layer thicknesses than the composite hood and brackets region. The behavior of the adhesives considered for use by DTNA are desired to be tested in temperature conditions that provide a realistic range of conditions DTNA products are to operate in. The temperature conditions of the geographical locations provide both warm and cold temperature deviations.

The study discussed here is composed of two phases of testing. In phase I, two adhesives provided by DTNA are tested against a range of temperatures. The specimens utilized in testing embody the mode I and mode II cohesive strength and toughness. In phase II, a design of experiments was incorporated to test the effects of

thickness, working time, and temperature against one of the adhesives provided. The process used in this study can help researchers and industries using these adhesives and experimental methods to have confidence in the parameters generated from the experiment to model adhesives. The study serves as a way to test the thickness, working time, and temperature effects of the environment on structural adhesives.

2. Literature Review

The literature review is divided into four subsections. Subsection one covers the origin of adhesives. Subsection 2 covers an outline of fracture mechanics leading into cohesive zone modeling. Subsection 3 covers cohesive zone modeling, traction separation laws, and relations of process zone size. Subsection four covers the parameters varied for the adhesives studied.

2.1 Adhesives Origin

The use of adhesives has been prevalent throughout history in both use and study. The earliest use of adhesives began around 4000 B.C., where tree sap was found to repair clay pots [9]. In 1500 B.C., the use of birch bark tar was used to fasten stones to sticks [10]. Antonio Stradivarius used adhesives to laminate the woods in his violins in the seventeenth century [9]. In the eighteenth century, it is found that the first patent was issued for a fish glue [9]. The previous examples of adhesives have all been of natural origins.

In the twentieth century, adhesives saw an improvement with the invent of synthetic adhesives [11]. The synthetic adhesive is not found in nature and produced by humans in laboratories. The majority of adhesives used in structural applications are synthetic adhesives. The number of components needed to begin solidification of adhesives can classify synthetic adhesives. One-component adhesives are found in single containers and require no mixings. The majority of one-component adhesives are moisture curing. Two-component adhesives have components that are stored separately in individual containers and require mixing of proper proportions to begin

solidification or curing. Many polyurethane, and epoxy adhesives are two-component adhesives.

The adhesive may have a physical or chemical cure. A physical cure occurs in pressure sensitive and contact adhesives. An example would be tape, band-aides, and patches. Chemical cure examples include polyurethane, epoxy, and acrylates. There is usually an associated cure time with both chemical and physical cures. The chemical cure time for adhesives usually has a working time when the adhesive has been mixed and is exposed to the environment, and a cure time where the adhesive is allowed to form completely. A good practice for adhering two materials together is for the adherents the adhesive is bonding together to be bonded and placed on a planar surface for the duration of the cure time before the end of the working time [12,13].

The study of adhesive behavior during use in service begins at the end of the cure time. At this time, the adhesive is at full strength, and recommended for use [12,13]. The adhesive is now part of the structure it is bonding and capable of holding its cured loading ability. The properties that represent the behavior for the adhesives to be modeled or designed with are based in the study of fracture mechanics.

2.2 Fracture Mechanics

The study of fracture mechanics begins with the observation that most failures begin with a crack. A crack may form from a defect in a material, a stress concentration located at a discontinuous location on a material, harsh environments causing thermal stresses, corrosion, and damage from fatigue, impact or unexpected loads. This crack can often lead to failures below a material's listed yield strength. This discrepancy is the motivation of fracture mechanics.

In 1913, Inglis discovered that the stress around a circular hole or corner was greater than the surrounding material [14]. Inglis was able to show the stress magnification of these areas depended on the radius of curvature of the hole using elasticity theory [14]. Where the stress concentration around an elliptical hole is found to be three times the applied stress [14].

Then in 1920, A. A. Griffith established a relationship to help explain brittle fracture [15]. Griffith based fracture from a potential energy approach, where the reduction in strain energy due to the formation of a crack must be equal to or greater than the increase in surface energy required by the new crack faces [15]. The fracture surface energy of the solid, greater than the free surface energy, can be derived into the strain energy release rate, which when equal to or greater than the surface energy creation rate, called the critical condition, leads to stable crack growth [15]. This approach is limited as the crack tip may become blunted or rounded due to plastic deformation at or around the crack tip, where there will no longer be a sufficient stress concentration, from the curvature of the crack, to continue the crack growth *i.e.*, the surface energy creation rate is greater than the fracture surface energy.

Irwin in 1948, then modified the Griffith criterion for brittle fracture to include a dissipative term [16]. Orowan also modified the Griffith criterion to include a local plastic dissipative term [17]. This dissipative term accounts for the stored elastic and surface energy of the material, and is used to describe the plasticity that occurs around a crack tip in non-brittle materials. Continuing with the study of fracture mechanics Irwin developed a method to describe the stress field ahead of a

crack tip, and the amount of energy available for fracture with a “stress intensity factor” [18].

The elastic energy release rate, G , of a material was discovered to be independent of the plastic zone size [19]. Indicating that an elastic solution alongside the unit area of crack in a material is sufficient to calculate the amount of energy available for fracture or increment of crack extension. Using this relation Irwin was able to relate the energy for crack extension to crack tip stress [18]. Irwin and Kies studied the concept of fracture resistance using an energy approach to describe the resistance a material has against crack extension against its crack length [20]. Irwin later revised this to show an increase in resistance as the crack progressed due to an increase in the plastic zone size [21]. This concept defines fracture instability by the critical energy release rate at the tangency of the resistance curve of the material, and the driving energy release rate of the material, G [21].

The methods discussed above show exceptional relations to describe brittle materials where any non-linear deformation of the material is confined to a small region near the crack tip. To analyze materials where large regions of the material are subject to plastic deformation before crack extension, Elastic plastic fracture mechanics (EPFM) is most appropriate. EPFM is based in crack tip opening displacement by Wells, and J Integral by Rice [22,23].

Crack tip opening displacement (CTOD) was originally crack opening displacement (COD), but was changed to distinguish differences from crack mouth opening displacement. The CTOD was proposed by Wells to extend the elastic stress

intensity factor approach into elastic-plastic yielding conditions [22]. The approach assumes fracture occurs when a critical CTOD is reached.

Rice, several years after CTOD had been published, in 1968 characterized the intensity of elastic-plastic crack-tip fields with the J integral [23]. The J integral is based on the deformation theory of plasticity, and is independent of the path of integration around the crack tip [23]. The J integral is used to describe the singularity intensity of the crack-tip stress field for elastic-plastic hardening materials, similar to the way the stress intensity factor is used to characterize the intensity of singularity of the linear elastic stress fields [23]. Hutchinson independently evaluated the character of crack-tip stress for both plane stress and plane strain conditions to reveal that the product of stress and strain varies as $1/r$ near the crack tip, and provided mathematical proof for this relationship [24].

Shih was able to provide evidence for a unique relation between CTOD and J integral approach that exists for a material [25]. Using a 2-D finite element analysis, Shih and German showed a factor between 25 and 50 is required to ensure a path independent J characterization of an annular region surrounding the crack-tip [25]. The analysis also showed that the J integral and CTOD relationship could be applied well beyond LEFM, where the yield stress can be replaced with the effective yield stress [25].

LEFM and EPFM are good at modeling materials where the presence of an initial crack leads to fracture. The methods are not as good at representing non-linear processes ahead of a pre-existent crack. Barenblatt and Dugdale in the 1960s

developed models to represent non-linear processes located at the front of a pre-existent crack [26,27]. Their work is the basis of cohesive zone modeling (CZM), which is created to study the region around a crack tip that has undergone plastic deformation to determine the possibility of crack extension and the direction of crack growth. CZM is able to predict the behavior of non-cracked structures, have large non-linear zones in model geometry, and can eliminate singularities of “infinite” stress that develop during mesh refinement in FEA. CZM’s ability to handle large non-linear zones suits the conditions an adhesive layer is expected to display between two rigid substrates when pulled in mode I loading for example. Where the size of the plastic deformation region that occurs in the non-cracked adhesive layer during load till fracture is expected to be out of the range of applicability of LEFM and EPFM.

2.3 Cohesive Zone Modeling

An agreement in the literature search conducted has found cohesive zone modeling (CZM) to be most appropriate for adhesive implementation into FEA [2,28,29]. The crucial aspect of CZM is that the fracture process zone can be described with a traction-separation law (TSL) relating the stresses and displacements in the adhesive zone, as the material properties degrade under load [28,30]. A mode I cartoon specimen with a fully developed process zone and traction separation law for that process zone can be seen in Figure 1. To utilize a CZM, the cohesive strength and toughness must be established. The cohesive strength and toughness for both mode I and mode II loading are the material properties needed for a CZM [29]. With mode I and II loading properties, the majority of loading scenarios a typical bond-line experiences can be modeled with confidence.

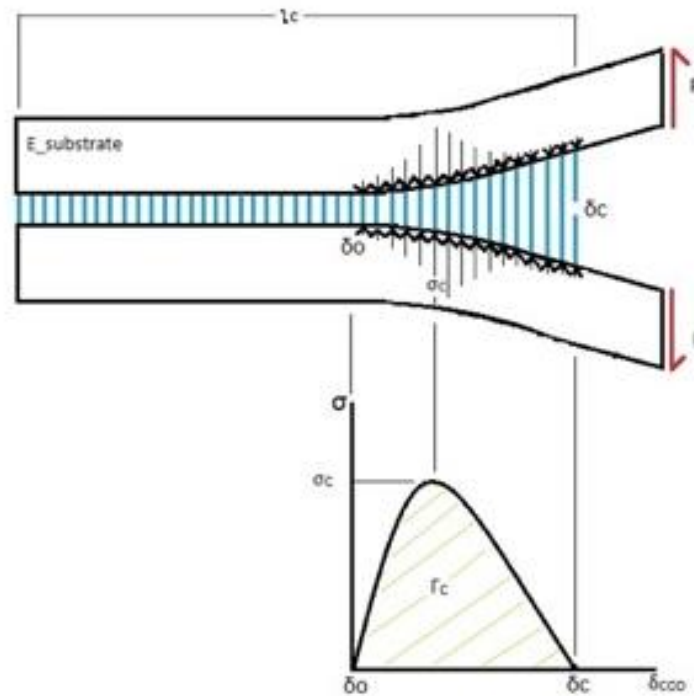


Figure 1- Traction separation law on a mode I tension specimen

In Figure 1, a cartoon adhesive joint specimen is shown experiencing load to first ligament failure in mode I loading. The specimen at the top of Figure 1 shows the regions of interest for adhesive specimens, namely the bond length, the adhesive process zone, and the substrate or adherent. A typical specimen contains two substrate materials on each side of the adhesive bond. Where the bond serves to join the two substrate materials. The adhesive bond length is represented by blue vertical lines acting as cohesive ligaments connecting the top and bottom substrate. The ligaments of a CZM span the adhesive region on a modeled specimen, and represent the adhesive behavior from onset of loading until failure, or critical crack opening displacement.

In the initial unloaded condition, the initial crack opening displacement, δ_0 , the initial crack length and the initial bond length, l_c , are all relaxed. As the specimen receives load in either mode I or mode II, the cohesive ligaments begin to degrade at the initial crack length interface. At this location, the largest deformation occurs at the ligament on the edge of the region. As the specimen is further loaded, the crack tip opening displacement and the process zone size increases. Their size expands until a critical crack opening displacement, δ_c , is reached [31]. At this point, the crack begins to form as the first cohesive ligament fails, indicating that the process zone is fully developed [31]. The fully developed process zone is the region of deformed cohesive ligaments that lead the crack tip. This critical displacement under continued load or displacement will continue to propagate through the ligaments in the direction perpendicular to the loading or displacement state in mode I loading. The critical crack opening displacement can be found for each mode I and mode II.

The cohesive strength, σ_c , of an adhesive is the ability of the adhesive region to carry load and return to its initial state with no deformation. The cohesive strength lies at the top portion of the elastic segment of a force-displacement curve. In testing the cohesive strength is usually the peak force the adhesive holds under load. The cohesive toughness, Γ_c , of an adhesive is the ability of the adhesive region to carry load until onset of failure, or crack propagation. The onset of crack propagation occurs when the bonded region reaches the critical separation energy required to begin degradation of the interface to zero. At this state, it is believed that a crack will grow, as the interface has no energy to support load. The area under the TSL is the

cohesive toughness. The cohesive strength and cohesive toughness can be found for each mode I and mode II.

The combination of these three elements make the ideal TSL. The strength, toughness and critical crack opening displacement in a fully developed process zone are interrelated. With two of the three parameters, the third can be calculated based on an ideal TSL. If the cohesive strength and toughness are known, the critical crack opening displacement can be calculated as it must lie at the end of an adhesive's cohesive toughness *i.e.*, when the adhesive has no energy to continue to support load. A fully developed process zone will include ligaments that are just beginning to deform, ligaments at max cohesive strength, and ligaments that have reached their cohesive toughness limit and fracture at the critical crack opening displacement.

The behavior of the cohesive ligaments along the bond-line are based on the TSL shape. Often the shape of the ideal curve is not the same shape of the experimentally-generated curve as the adhesive behavior can take on a few different forms. For example, if the interface material the adhesive is bonded to is changed the adhesive may act brittle, and the change from the elastic region to the plastic region and decay of the adhesive may be extremely sharp. That is to absorb little separation energy after the cohesive strength is met. This scenario would result in low cohesive toughness values, which would change the overall shape of the TSL. Depending on the substrate material different TSLs can be generated for the same adhesive.

Once the process zone has been fully developed the deformed region remains the same size until complete failure of the bonded area, under the same continuous

loading state. The process zone length or fracture length scale relative to the total bond length indicates the type of failure that prevailed [31]. This relationship can be described by the value of a dimensionless group, seen in inequality 1, where E is the elastic modulus, Γ is the cohesive toughness, σ is the cohesive strength, and l_c is the bond length [31].

$$\text{Strength Dominated : } 2 \ll \frac{E\Gamma}{\sigma^2 l_c} \ll 0.1 : \text{Toughness dominated} \quad (1)$$

This inequality describes if the fracture length scale is strength or toughness dominated, or a mixture of both. For large values, greater than approximately 2, of the dimensionless group, the fracture load begins to converge to the fracture load predicted by strength based failure criterion. Where in this case the fracture event depends only on modulus, geometry and cohesive strength. The fracture of the region in this case is considered strength dominated for these values [31]. For small values of the dimensionless group, less than 0.1, the fracture load converges to the fracture load predicted by linear elastic fracture mechanics [30]. In this case, the fracture event depends only on modulus, geometry, and toughness. The fracture is toughness dominated in this case [31]. For values between the extremities, the cohesive strength and toughness of the region are important to fracture development.

By utilizing specimen geometry to achieve small or large values of the dimensionless group the strength or toughness of a region can be determined accordingly. Test methods that use tension or compression specimens provide a starting point for the numerical fitting procedures of these parameters [32,33]. The

values for these TSL are also material and loading rate dependent [6]. TSL can be created for any of the loading modes, or a mixed mode loading condition. The study here will find properties that can be used for individual mode I and mode II TSLs.

2.4 Adhesive Parameters

The influence of the environment has been shown to influence adhesive behavior [2,5,28,34,35,36]. Kang [2], Xuan [5], and Banea [28] studied temperature conditions on adhesives and found decreased performance effects. Carbas [34] studied the effect of different adhesive cure states on the strength and stiffness of adhesives and found decreased performance with increase of temperatures above the glass transition temperature of the adhesive. Ahmad [35] conducted several studies finding when adhesives have been soaked in water a linear decrease in strength is found, and noted decreased performance near the glass transition temperature. Budhe [36] studied pre-bond moisture in adhesives finding that with increased time to dry the adhesive is less effected as measured with fracture toughness tests. The previous studies and findings suggest the temperature deviation the specimens are subjected to in service across varying geographical locations will influence adhesive properties.

Adhesive thickness is often portrayed in manufacture data sheets as a range [12,13]. This range sometimes includes an optimal thickness [13]. However, there is usually not a reported strength for the optimal thickness and the more general range. The difference in loading capabilities is left for the user of the adhesive to determine if the load carrying ability is suitable for the adhesives task [12,13]. In Imanaka's work [37], it is stated that an increase in the adhesive layer thickness enlarges the range having non-uniform stress distributions, resulting in lowering of the adhesive

strength. Imanaka studied thicknesses of 0.05, 0.1 and 0.5 [mm], and found a decrease in endurance limit of butt, scarf and butterfly type joints with increasing adhesive layer thickness [37]. In Marzi's work [6], thicknesses of 0.2, 0.5, 1.0, 2.0, and 4.0 [mm] are studied and found increased variability with increasing thickness.

The literature review conducted throughout the course of this study did not reveal any applicable adhesive working time studies. The studies found for working time variation with adhesives often related to adhesives used in dentin structures, and increasing the priming time of the adhesive [38, 39]. Adhesive working time is nominally given a value to not be exceeded by manufactures.

These parameters can be observed from measured load and displacement data for each condition and loading mode from a specimen that embodies the parameter of interest. In phase I of testing four specimens will be used to embody the mode I strength, the mode I toughness, the mode II strength, and the mode II toughness. These specimens will be exposed to various temperature conditions. In phase II, the working time will be varied to produce a recommended and expired application time, and a thin and thick thickness will be exposed to various temperature conditions. The specimens manufacturing, analysis, and origin are discussed in the materials and method section.

3. Materials and Methods

The materials and methods section is split into two subsections. The first subsection will introduce the specimens in test ready form, and present their analysis. The four specimens to be described in the first subsection are for measuring the mode I cohesive strength, mode I cohesive toughness, mode II cohesive strength and mode II cohesive toughness. Subsection 2 will describe the manufacturing and testing steps. In the steps; the manufacturing, the adhesives selected for the study, how the environmental conditions were tested, how the thickness was varied in Phase II, how the working time was varied in Phase II, how the adhesives were bonded, cured, and loaded, and monitored during temperature testing, will be described.

3.1 Test Ready Specimens

The specimen that represents the mode I cohesive strength in this study is a uniaxial dog bone tensile specimen (DBTS). The DBTS specimen can be seen in Figure 2. The DBTS specimen has aluminum substrates bonded on the outer region of the center. The central crack of the desired size is created using polytetrafluoroethylene (PTFE) tape to cover the region that is not to be bonded. The geometry of the bond length is selected based on a strength dominated fracture length scale. The sample is tensioned from the loading holes and the peak load is used to calculate the cohesive strength using the standard equation for stress, $\sigma = F/A$, where F is the peak load and A is the initial area of the bond.

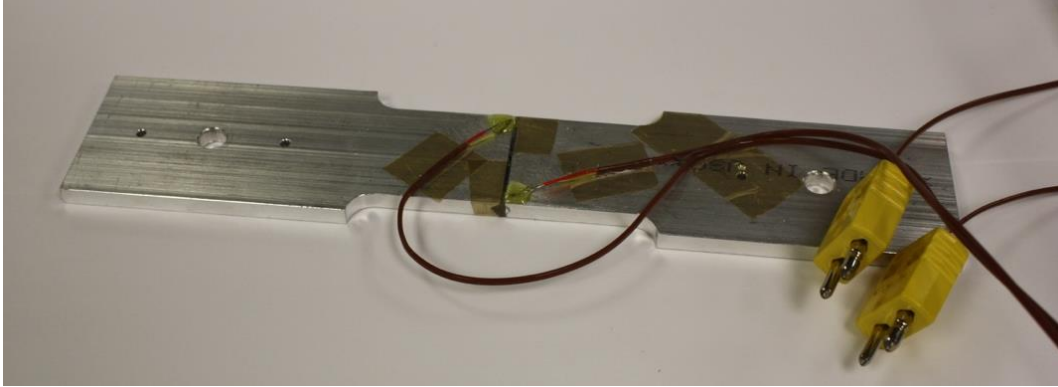


Figure 2 – DBTS test specimen ready for testing

The specimen that represents the mode I cohesive toughness in this study is a dual cantilever beam (DCB) [40,41]. The geometry of the bond is selected based on a toughness dominated fracture length scale. The DCB specimen can be seen in Figure 3. The DCB specimen has aluminum substrates that are bonded in the center. The desired bond length is created with PTFE tape at the beginning of the bond on loaded end. The specimen is loaded with pins through the loading holes in tension. The peak load is used in an equation for the energy release rate, G , shown in Equation 1, which is a function of the transverse loading (F), crack length (a), modified modulus ($\bar{E} = E / (1 - \nu^2)$), where E and ν are substrate modulus and Poisson ratio respectively, and beam thickness (h) [40].

$$G = \frac{12(Fa)^2}{\bar{E}h^3} \left(1 + 0.674 \frac{h}{a}\right)^2 \quad (1)$$

The energy release rate can be related to the cohesive toughness. It is in good agreement that symmetric DCB specimen will provide the mode I cohesive toughness [40,41].



Figure 3 – DCB specimen ready for testing

The specimen that represents the mode II cohesive strength in this study is the double lap shear specimen (DLS) [42]. The geometry of the bond is selected based on a strength dominated fracture length scale. The DLS specimen can be seen in Figure 4. The substrate is made of aluminum. The specimens are loaded into self-tightening grips in a shear loading state [43]. The peak load value is used to calculate the cohesive mode II strength. The equation for strength is the same used in mode I, $\sigma = F/A$.

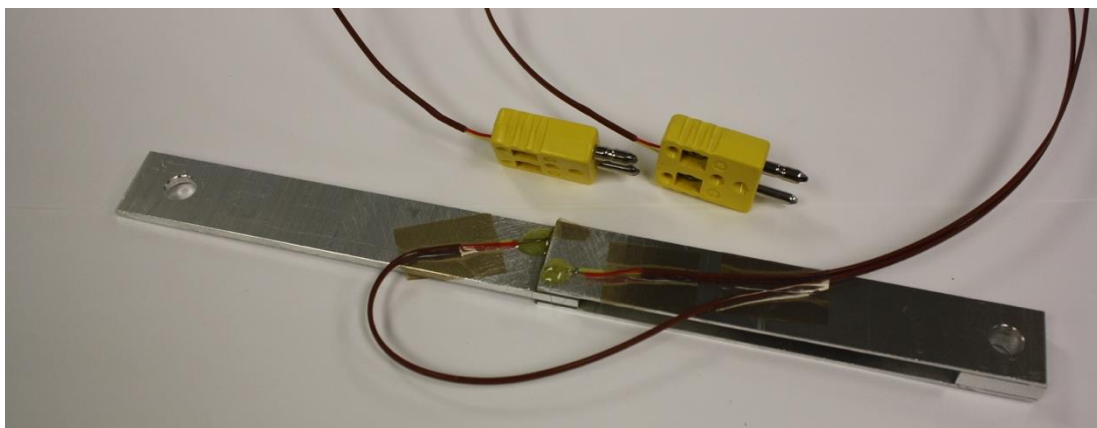


Figure 4 – DLS specimen ready for testing

The specimen that represents the mode II toughness in this study is the shear loaded dual cantilever beam (SLDCB). The specimen is a variation of the work by Marzi et al. [6]. The SLDCB specimen can be seen in Figure 5. The SLDCB substrate is made from aluminum. The SLDCB specimens are loaded into a shear loading fixture that uses compressive force from the cross head on a universal testing machine to load the sample in shear along the bond line. The geometry of the bond is based on a toughness dominated fracture length scale. To obtain the cohesive toughness, Equation 2 below from Tada's book was used [44]. This involves a stress intensity factor and bulk modulus. The stress intensity factor is dependent on loading, crack conditions, and a geometry correction factor.

$$G = \frac{K^2}{E} \quad (2)$$

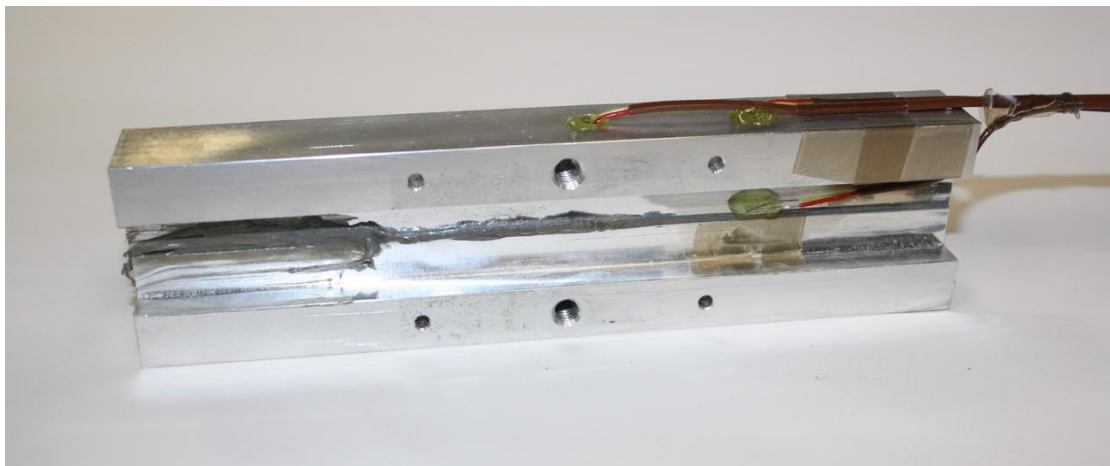


Figure 5 – SLDCB specimen ready for testing.

The adhesive properties that these specimens provide can then be used harmoniously with cohesive zone modeling to model how adhesive joints ideally behave under degradation [6,29,32].

3.2 Manufacturing and Testing Steps

The specimens used for testing were manufactured in house at Oregon State University (OSU) in the Machine Realization Production Laboratory. The specimens from stock order to test had ten major steps. The steps will be discussed in order of occurrence, and methods relevant to each step will be discussed as needed. Additional information for these steps that does not need immediate attention can be found in the appendix. The methods presented related directly to the experiment.

The specimen testing was completed in suites for Phase I. A suite contained the specimens from a single loading mode. Triplicates for each mode's loading condition were tested at each temperature. For example, the DCB and DBTS specimens would be combined into a suite and likewise the SLDCB and DLS specimens. A total of 18 specimens would be in a suite. Phase I testing was comprised of four suites. Two suites for each Adhesive selected in phase I too test both mode's loading conditions against the temperatures chosen. In Phase II, a suite contained a variation of recommended and expired working times for DCB and SLDCB specimens at a single bond thickness. Phase II testing was comprised of six suites, with 12 specimens in a suite. A suite of testing was manufactured with the following steps.

The **first** step in production of test specimens for adhesive testing is to order raw materials. The materials needed for the experiment on adhesive testing are the substrate, the adhesive, the adhesive application device, cleaning materials, mold release, bond line fixtures, surface abrasion sheets, and non-adhering tape, or TPFPE tape. Most materials are available from McMaster-Carr [45]. The stock for the substrates is purchased to best resemble an un-featured half specimen. The DCB and SLDCB specimens used the same 7/8" inch 6061-T6 aluminum square stock purchased in 5' sections. The stock for the DLS specimens was purchased in 20" by 20" sheets. The stock for the DBTS specimens used 2.5" by 1/4" thick stock purchased in 5' sections. The stock would then be cut according to the estimated bond lengths needed. A bill of materials for needed items can be found in the appendix. Once the materials needed have been obtained, the subsequent steps may be produced.

The **second** step is for the specimens to be manufactured from raw stock. The raw material stock is first rough-cut according to the feature needs of the specimen. The stock was primarily rough-cut with a horizontal band saw. A vertical milling machine would then be used to get the rough-cut stock down to the required size and produce a smooth edge surface finish. The size for DCB and SLDCB specimens was used to create a fixture for manufacturing the loading, fixture, and alignment holes. A picture of the raw stock for specimens ready for this machining can be found in the appendix. The sheet drawing for the specimens can also be found in the appendix.

The manufacturing of test specimens was desired to be quick and repeatable. To meet this outcome a custom Computer Numerical Control (CNC) manufacturing

fixture was designed, built, and implemented to ease DCB and SLDCB manufacturing. A previous CNC fixture for the DBTS specimens was adopted and modified to be used. The DCB and SLDCB CNC fixture can be seen in Figure 6. The DBTS CNC fixture can be seen in Figure 7. The fixtures made numerous hours of machining into a manageable workload.

The fixtures for the DCB specimens installed directly into the CNC with two in-slot bolt fasteners on opposing sides. The DCB stock would then be placed directly into one of four slots in the fixtures and held in place with a restraining bar. The DBTS fixture installed into a standard vice, and was restrained with a 1/4-20 bolt and washer. The DBTS fixture was used to manufacture the curved geometry of the specimen and produce the needed distance for the adhesive thickness desired in later bond-line fixtures. Three fixture holes were placed with CNC code prior to installment of a DBTS specimen into the DBTS CNC fixture. The fixture's corner would then be located and four specimens, two top and two bottom halves, for the DCB fixture or a half DBTS specimen could be manufactured until the desired specimen count was achieved. The specimens were cleaned with simple green post manufacturing.

The specimens once removed from the CNC fixture are washed in a separate bath with a simple green and water mixture. A ratio of 1 oz. simple green to 5 gallons of water was used. The simple green is a solvent that removes the oils and coolant used in manufacturing. The specimens are then rinsed with water and set aside for a water break test [46].



Figure 6 – DCB and SLDCB CNC fixture

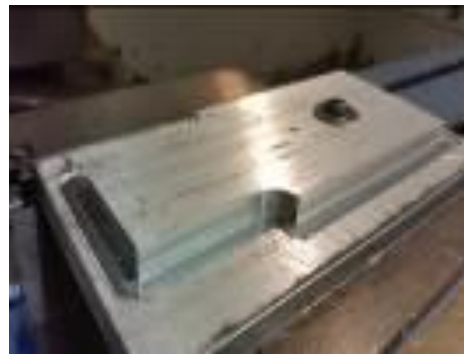


Figure 7 – DBTS CNC fixture

The DLS specimens were made according to ASTM standard [42]. The only manufacturing that needed to occur for DLS specimens was drilling the alignment holes to be used with the curing fixture plate. A plate with alignment holes for the edge specimens of the DLS sheet held the specimens in place for curing. The sheet was placed with shims to ensure proper bond thickness. The DLS specimen plate can be seen in Figure 8. The bond length was controlled with PTFE tape. The bottom plate would be placed on the fixture, and first adhesive layer applied, the middle plate

would be placed and second adhesive region applied, and the last plate would be set on the middle plate, and a small weight applied to the top of the sheet to ensure good adhesion.

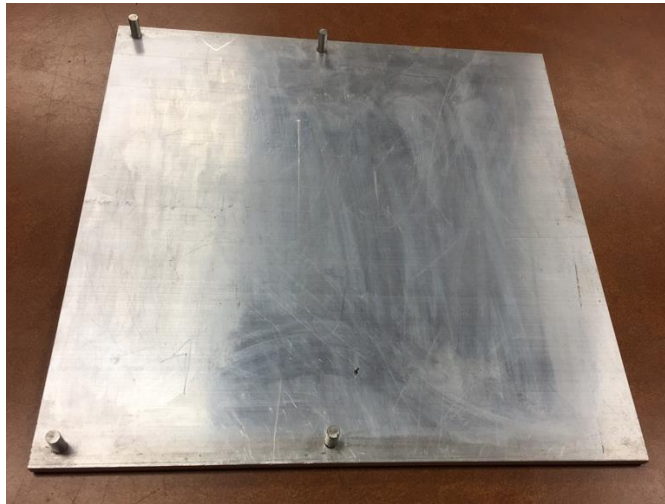


Figure 8 – DLS specimen fixture

The **third** step is to abrade the adhesive surface on the specimens to be prepped for the adhesive application. The surface for the adhesive is cleaned and mechanically abraded for increased adhesive contact. The specimens are dried from the water break test and rinsed with isopropanol alcohol and set aside under laboratory conditions to dry. A crosshatch abrasion method is applied with 10 passes of a sanding block in one direction followed by another rinse of isopropanol alcohol to remove any aluminum (substrate) dust from the abrasion process. This step is repeated in a direction perpendicular to the previous. This is done twice, first with 120 grit sand paper then followed by 60 grit sand paper. The process above for abrasion was suggested by the manufactures to achieve good results with the substrate used [12,13]. The surface roughness of the adherent has been shown to enhance the

wettability of the adhesive [47]. The specimen is then allowed to dry, and ready for subsequent steps.

3.3 Pliogrip Prep

The Pliogrip specimens had a few additional steps for manufacturing. The additional manufacturing steps came from a desire to test the specimens against a composite material provided by DTNA. The material was 3 mm thick and in sheets of 500 mm² size. A sandwich specimen was created using the specimens described. A layer of the composite was bonded to each aluminum substrate. The Pliogrip specimens can be seen in Figure 9. The aluminum substrate had 5 mm removed from the surface, on the adhesively bonded side, to compensate for the added composite material layer and the additional adhered region between the composite and the aluminum. These two substrates were then bonded by a smaller bond region in the middle, whose thickness matched the bond thicknesses of the Plexus specimens.



Figure 9 – Pliogrip specimens with layer of SMC

These specimens were designed to replicate the original specimens, with an added interest in the interaction between Pliogrip and the composite sheet material (SMC). To capture similar behaviors of the original specimens, the failure region had to be between the sheets in the middle adhesive region. PTFE tape was used to reduce the width of the bond length for this situation to occur. The amount of material removed to account for the two added layers of SMC, matched the needed distance on the bond fixture plates, so the bond thickness in the middle of the sandwich specimen matched the Plexus specimens.

The surface prep on the SMC for Pliogrip was different from the aluminum substrates. No abrasion on the SMC was done. The SMC was made of fibers and molding. Abrasion to the surface would almost guarantee the Pliogrip adhesive would fail in the substrates. Additional to this no surface abrasion is done by DTNA in the manufacturing process with this material. The surface prep matched Plexus in terms of intermediate cleaning between steps, and water break test application to ensure a clean surface.

The **fourth** step for the specimens is to be prepped for adhesive application. TPFPE tape is applied locally to regions where the adhesive is not to bond. The non-bonded region serves to control the bond length of the specimen. The bond length for the DBTS specimen was 5 [mm]. The bond width for the DBTS specimen was 6 [mm]. The bond length for DCB specimen was 100 [mm] for Plexus, and 90 [mm] for Pliogrip. The bond width for DCB specimen was 22 [mm] for Plexus, and 10 [mm] for Pliogrip. The bond length for DLS specimens was 25.4 [mm] for Plexus and 10

[mm] for Pliogrip. The bond width for DLS specimens was 25.4 [mm]. The bond length for SLDCB specimens was 172 [mm] for phase I Plexus testing, 160 [mm] for phase II plexus testing, and 110 [mm] for Pliogrip. The bond width for SLDCB specimens was 5 [mm]. The specimens are rinsed with isopropanol alcohol before and after application of TPFPE tape. Once the surface has dried, the adhesive is ready to be applied.

The **fifth** step for the specimens is to apply the adhesive. The adhesives chosen for the study are Plexus MA832, an adhesive considered for structural cab application, and Pliogrip 7700/220b, an adhesive considered for the truck hood assembly. The adhesives for testing were provided by DTNA.

Plexus MA832 is a two-part methacrylate designed for structural bonding of unprimed metals as well as composites with little to no preparation of the bonding surface. The adhesive is mixed at a 10:1 ratio immediately before application and is advertised as having high strength, great fatigue properties, and good toughness. Plexus MA832 comes in 380 ml cartridges, 5-gallon pails, and 50-gallon drums [12].

Pliogrip 7700/220b is a two-part urethane adhesive designed to bond composites, coated metals and concrete among other materials [13]. This adhesive is mixed in a 1:1 ratio immediately before application and is advertised to have well balanced mechanical properties and impact toughness [13].

Both adhesives were applied in an ambient lab environment of 20°C and a relative humidity of 65%. A mixing nozzle mixed the adhesive in the proper ratio in combination with an adhesive gun that was specific to the adhesive tube. The

adhesives used had a working time of ~15 minutes. The adhesives on average were in the bond line fixtures for curing before half of the working time had expired. In Phase II the expired working time was tested by applying the adhesive to the bottom substrate and then waiting until 10 [min] had passed from the recommended working time before the top substrate was placed, and the bond line fixture applied.

The **Sixth** step is to set the specimens into the curing bond line fixtures. The bond line fixtures were made from 6061-T6 aluminum stock, and had 6 manufactured holes, three at the top and three toward the bottom. The corner holes had 1/8" diameter steel pins of 1/2" length press fit into the holes. The middle hole of two pins would align a 1/4-20 screw. The alignment pins would insert into slip fit holes on the specimen and penetrate 1/4" into the alignment hole. Once the top and bottom alignment holes were attached to the upper and lower segments of the specimen a screw would be twisted into its hole and the fixture-specimen assembly placed on a planar surface. There were six DCB and SLDCB fixture plates made, and four DBTS fixture plates made. This amount allowed an entire suite of specimens to be made for testing.

The bond line fixtures were sprayed with mold release in a separate location prior to bonding the specimen. The release ensured the adhesive would not adhere to the fixtures. The DCB and SLDCB fixture plate can be seen in Figure 10. The DCB and SLDCB fixture plate held the bond thickness at 0.6 [mm] for phase I testing. The DBTS fixture plate can be seen in Figure 11. The DBTS fixture plate held the bond thickness at 0.6 [mm] for phase I testing.



Figure 10 – DCB, SLDCB bond line fixture on an SLDCB specimen



Figure 11 – DBTS bond line fixture

The adhesive bond line fixtures were made as a substitute to creating the SLDCB, DCB, and DBTS specimens from being created in sheets. The DLS specimens were prepared with the sheet method and required no bond line fixtures, but would need to be physically separated into specimen coupons once cured for the recommended time. The change from the sheet method to the bond line fixtures was to represent more industrial styles of adhesive application and to increase the ability

to control the bond line thickness in individual samples. The change also requires less machining to occur post bonding, as the loading holes, and curved geometry regions would not be able to be manufactured prior to cutting the specimen from the sheet. Meaning the bond would undergo machining forces from these actions, and possible contamination from any coolant fluids. The alternative to this is drilling partial top holes in the sheets where loading tabs can be screwed into, this process is time consuming during testing, as there can be no slip in the loading tab. The sheet method may also require the use of small beads with a diameter equivalent to the bond line to prevent any sagging in the bond line in the middle segments. These beads would create regions in the adhesive where testing could be compromised from physical interstitial beads in the adhesive matrix. The cutting of the sheets was also a cost driving effort. The cutting of the cured sheets requires a blade or process that did not mind cutting the adhesive layer sandwiched between the aluminum substrates, and in the case of Pliogrip, an additional composite sheet material layer.

In Phase II, the thickness was varied by milling the adhesive from the previous testing away, as the substrate was not damaged during the testing of the adhesive. The milling process varied the thickness of the bond slightly between each specimen but between thin and thick bonds the specimen bond thickness had an average deviation of 0.507 [mm]. The thin bonds had an average bond thickness of 1.27 [mm]. The thick bonds had an average bond thickness of 10.38 [mm]. The adhesives were given a full 24 hours to cure, and tested with the next 24 hours. The adhesives cured on a planar surface in an ambient laboratory environment.

The **seventh** step is to apply thermocouples to the specimens to be monitored during testing in the temperature chamber. The specimens had a minimum of two thermocouples placed near the bond line to ensure the temperature of the specimen was at the desired state. The DCB and SLDCB specimens were long enough to have a third thermocouple placed near the bond line on the substrate. The thermocouples plug into a connection inside the temperature chamber that was read into a LabVIEW program to monitor and collect temperature values. The thermocouples were epoxied with a two-part hobby adhesive, and the cord tapped to the specimen with TPE tape, so the bond line could be viewed from the testing window. The thermocouple placement for the DCB, DBTS, and SLDCB specimens can be seen in Figure 12.



Figure 12 – Thermocouple placement on DCB, DBTS, and SLDCB specimens

The **eighth** step is for the specimens to be placed into the loading fixtures. The chamber was made to accommodate the fixtures needed for testing. The chamber is 42” tall, 19” wide, and 30” deep [48]. The shear fixtures for strength require 38” of height to conduct a test, and the toughness fixture is 15.5” wide. The chamber had

loading extenders for the testing fixtures. The loading extenders were made of stainless steel, and extended from the bottom and top of the Instron base, and cross head fixtures, into the chamber through a double seal. The loading extenders had different lengths to accommodate the different fixture heights required to test the specimens. The loading extenders can be seen in Figure 13.



Figure 13 – Steel loading extenders for the loading fixtures.

The specimens used three different loading fixtures for the testing. The DCB and DBTS specimens used the same loading fixtures. The DCB and DBTS loading clevis can be seen in Figure 14. The DCB and DBTS loading clevis had a pin connection to the loading cell or base of the Instron on one side and another pin connection to the specimen on the other. The specimen was held in place with pins that were inserted through the grips that lied on each side of the specimen in a U shape as seen in Figure 14. The internal pins helped to center the specimen under the loading plane.



Figure 14 – DCB and DBTS loading fixtures.

The DLS Instron grips post a -30°C test can be seen in Figure 15. The DLS specimens for mode II strength used Instron self-tightening grips [43]. The overlap of the specimen and the grips is 1". The grips would be applied onto the specimen by first placing the specimen into the bottom grips and gradually tightening the specimen into place. The top grips would be place onto the specimen in the loading portion of the specimen and tightened onto the specimen. A pre-load of 100 [N] was applied to the specimens to ensure the bond was not damaged, and the specimen was securely in the grips.

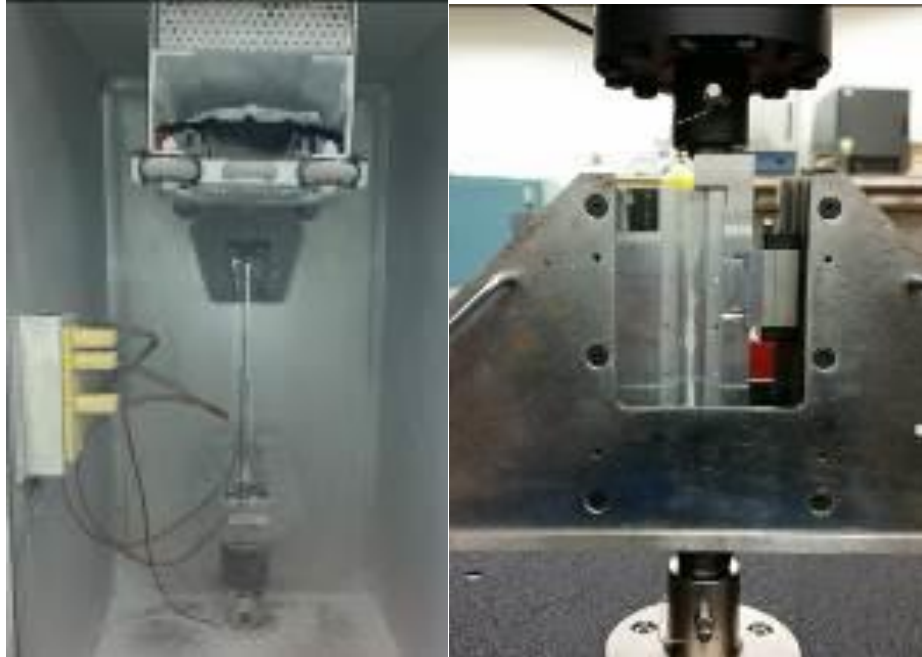


Figure 15 – left- Self-tightening grips for testing DLS specimens in the temperature chamber at -30°C in the Instron testing machine

Figure 16 – right - Shear loading fixture for testing the SLDCB specimen in the Instron testing machine

The SLDCB specimens used a fixture from previous researcher's work [29]. The SLDCB fixture can be seen in Figure 16. The SLDCB specimens were placed into the loading fixture on a region with guided tracks for the specimen and a top slide that would cover the right side of the specimen as pictured. The fixture had a loading block placed under the left side that allowed the right side to travel downward under a compressive force.

The **ninth** step is for the specimens to be placed into the temperature chamber and brought to the required temperature for testing the environmental conditions. The cold temperature was selected at -30°C , a temperature that a winter condition is capable of producing. The warm temperature was selected at 45°C , a temperature that makes cloud shade feel 10°C cooler on a typical desert summer day. A room temperature of 20°C was selected for a comparison of the extremities. These temperatures were tested against the adhesives described earlier for phase I testing. In phase II, the temperatures were varied slightly to -20°C , 20°C , and 40°C . The change in temperature reduced the testing time significantly. The environmental conditions selected for testing simulate the real-world conditions that the trucks produced by DTNA operate.

The room temperature specimens were loaded into the testing fixtures and tensioned or compressed till failure without the use of the temperature chamber, as the ambient lab conditions fell within the range needed to test [1]. The specimens at varied temperatures were loaded into a pre-cooled or heated chamber, the pre-load applied, and chamber resealed and held for further temperature change to the desired state.

This range of temperatures would be provided by a custom in-house built temperature chamber that attaches onto an Instron testing machine. The temperature chamber, heat exchanger unit, and the Instron testing machine that it attaches too can be seen in Figure 17. The performance, build parameters, and specifics of the chamber can be read in Meraz's work [49].

The chamber utilizes a heat exchanger unit that pumps fluid through a tube and fin heat exchanger mounted inside the double walled stainless-steel insulated chamber. The heat exchanger fan assembly blows air down toward the specimen in the chamber, heating or cooling the specimen to -30°C , -20°C , 40°C or 45°C , respectively for the test. The heat exchanger unit is made by Julabo, and the heat exchanger by Flex-a-Lite [50, 51]. Together this system was able to provide the temperature range needed for testing the environmental conditions on the adhesives.



Figure 17 – Temperature chamber built by Meraz at Oregon State University

The chamber temperature was set on the heating and cooling circulator. The circulator passes fluid to the heat exchanger, where the addition or removal of heat

occurs in the chamber. The circulator can be seen in Figure 17. The heat exchanger can be seen at the top of Figure 15. The placement of the heat exchanger was designed to have the fan assembly blow the air surrounding the heated or cooled fluid in the heat exchanger directly on the specimen for optimal convective heat exchange.

The test specimens were heated or cooled to the required temperature and held for a minute to ensure a stable environment. The temperature and relative humidity during the testing was monitored in LabVIEW. The thermocouple from the specimens plug directly into a connection panel inside the chamber. In Figure 15 the connection panel can be viewed. An extra thermocouple was plugged into the connection panel for a comparison of readings between the specimen, and heating and cooling circulator output. Under the connection panel and in the rear of the chamber the two analog humidity sensors were mounted.

The **final** step is to test the specimens. An Instron testing machine was used to apply a constant crosshead rate of 2.5 mm per minute. The rate was selected following the procedure of ASTM standard [42]. The rate places the adhesive fracture in a quasi-static loading condition. The loading condition in this range is able to capture the initial parameters for the traction separation law used for modeling adhesives. The DCB, and DBTS had a cross head displacement in the tension direction perpendicularly away from the bond line. The DLS, and SLDCB had a crosshead displacement parallel to the bond line and in the tensile and compressive direction, respectively.

4. Results

The results from the experimental tests will be presented in this section, in the order of Phase I and then Phase II. In Phase I, the Mode I cohesive strength, Mode I cohesive toughness, Mode II cohesive strength, and Mode II cohesive toughness, from Plexus and then from Pliogrip will be presented. Following this the Phase II testing with Plexus for Mode I cohesive toughness, and Mode II cohesive toughness will be presented. The figures provided here are displayed in force [N] and displacement [mm], as recorded from the Instron universal testing machine. The cold temperature specimens in the light gray solid lines, the room temperature specimens in the medium gray solid lines, and the hot temperature specimens in the dark gray solid lines. Above the force and displacement figures, there are bar charts, of the results. Following the individual specimen results will be tables of the results, where the forces and displacement from testing were used with the initial specimen's bond area to give the engineering values of strength and toughness as described in the materials and methods section. After the tables will be a statistical analysis from Phase I and then Phase II. The next section will be a discussion of the testing results.

Phase I - Plexus

In Figure 18, the results for the dog bone tensile specimen for Mode I strength bonded with Plexus can be seen.

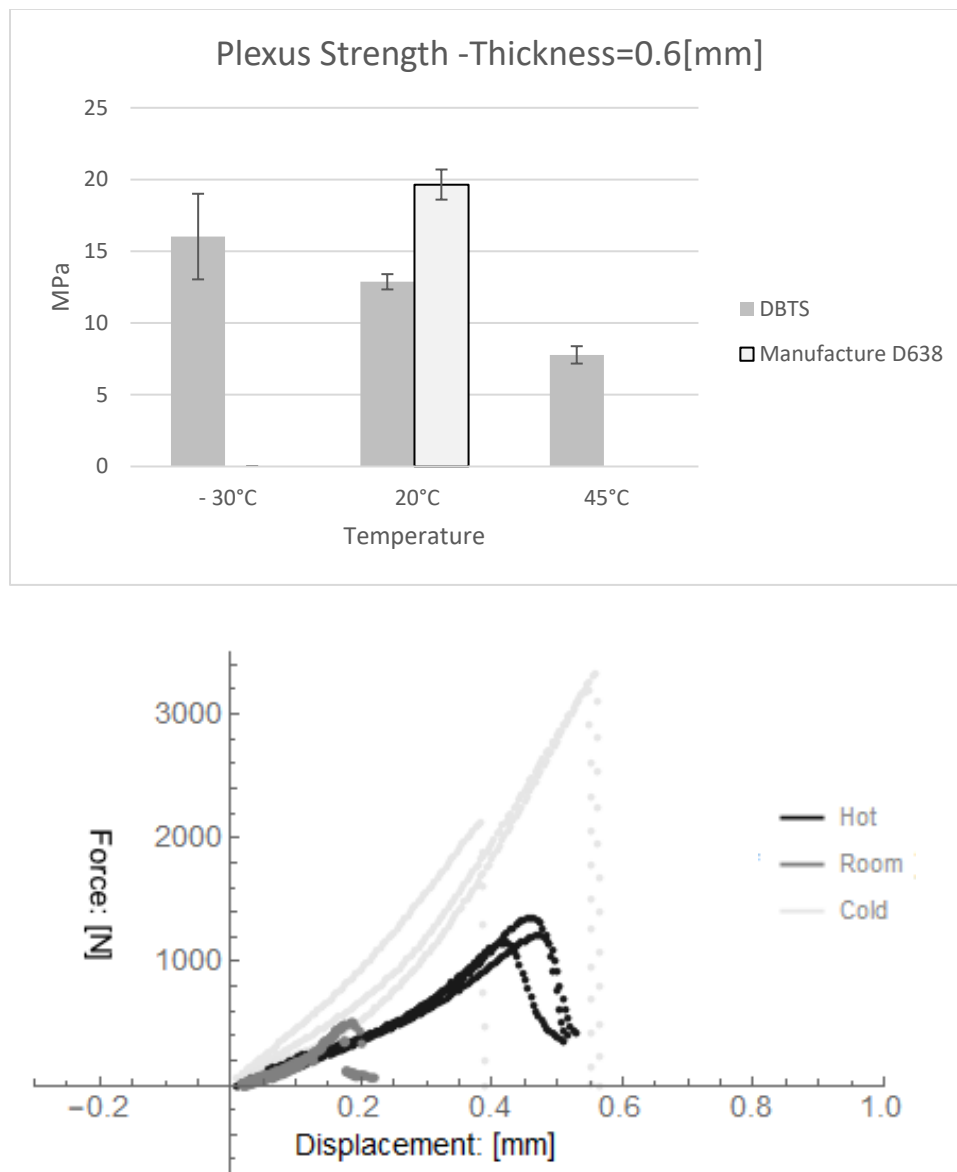


Figure 18 – DBTS specimen results

In Figure 19, the results for the dual cantilever beam for Mode I toughness bonded with Plexus can be seen.

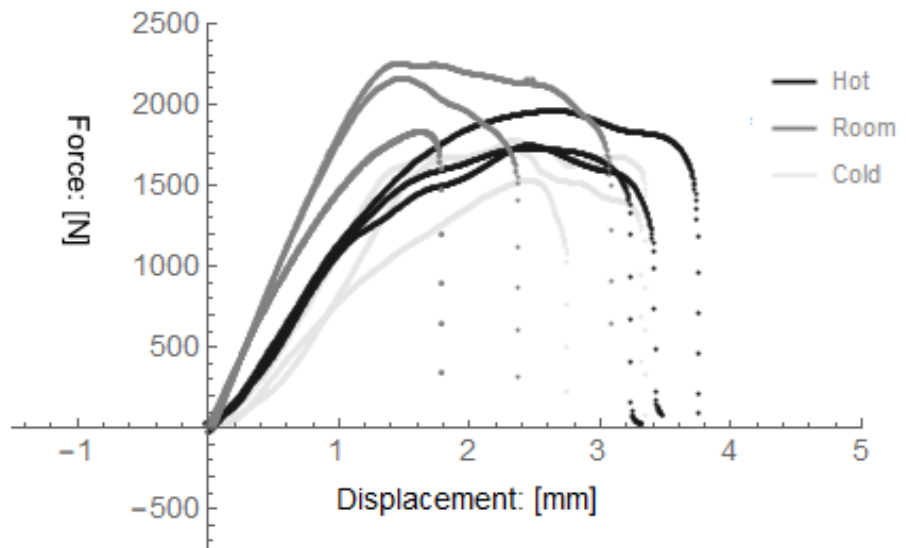
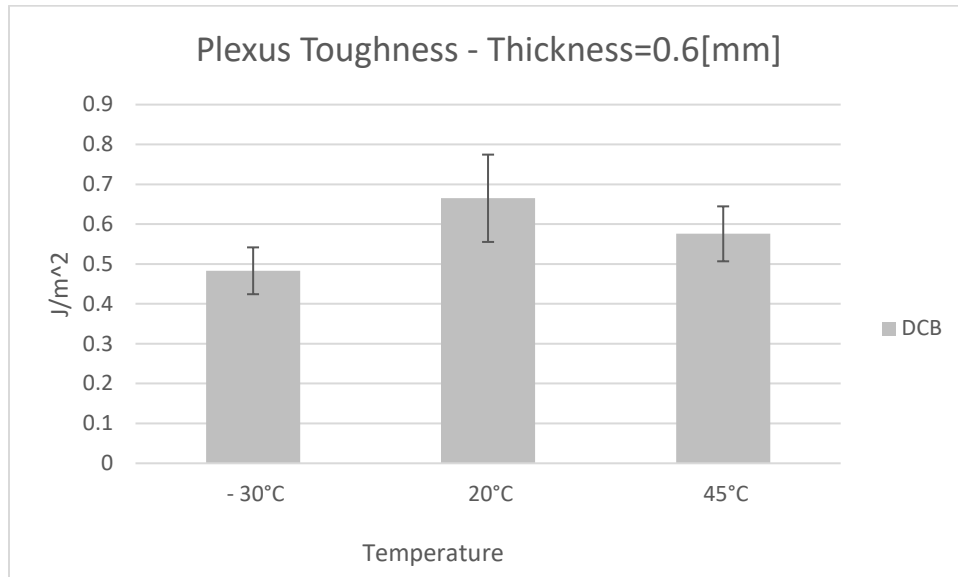


Figure 19 – DCB specimen results

In Figure 20, the results for the double lap shear specimen for Mode II strength bonded with Plexus can be seen.

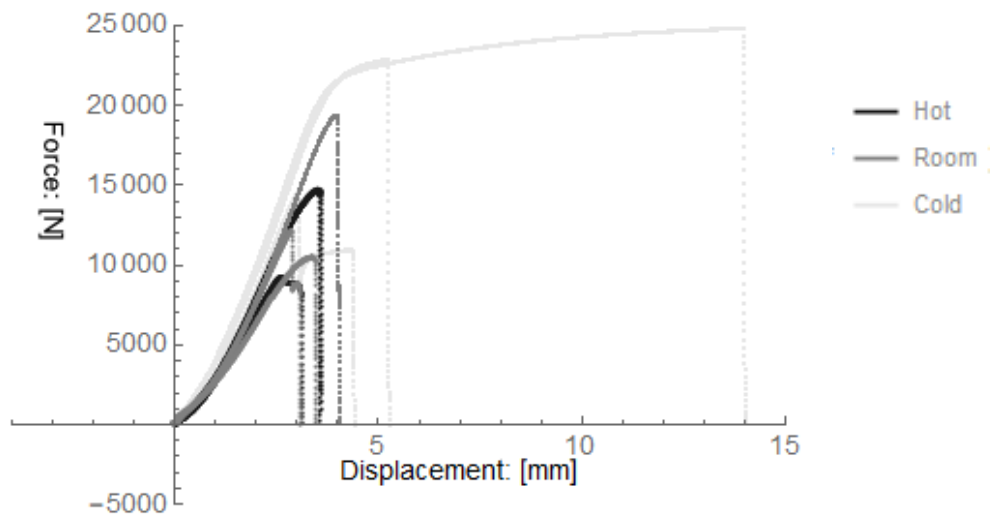
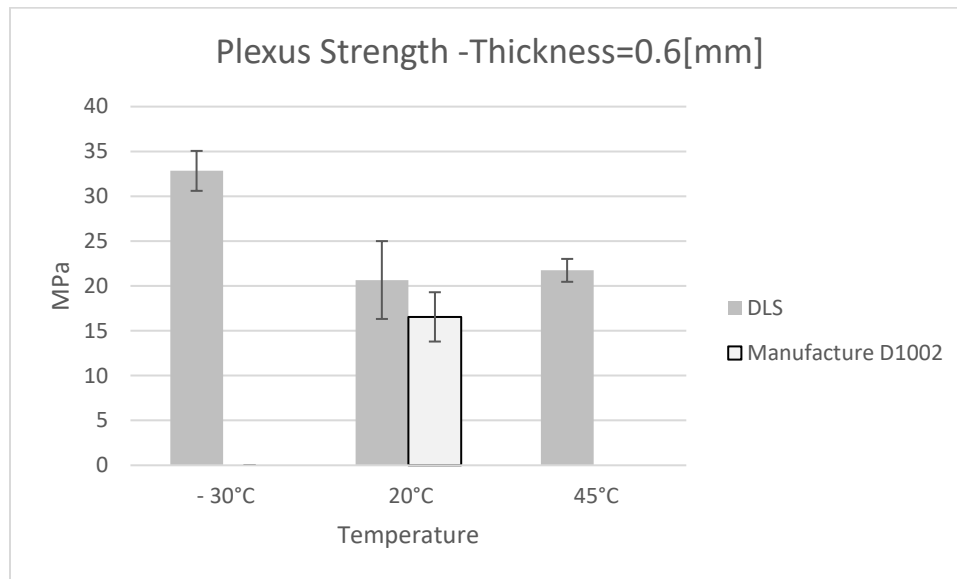


Figure 20 – DLS specimen results

In Figure 21, the results for the shear loaded dual cantilever beam specimen for Mode II toughness bonded with Plexus can be seen.

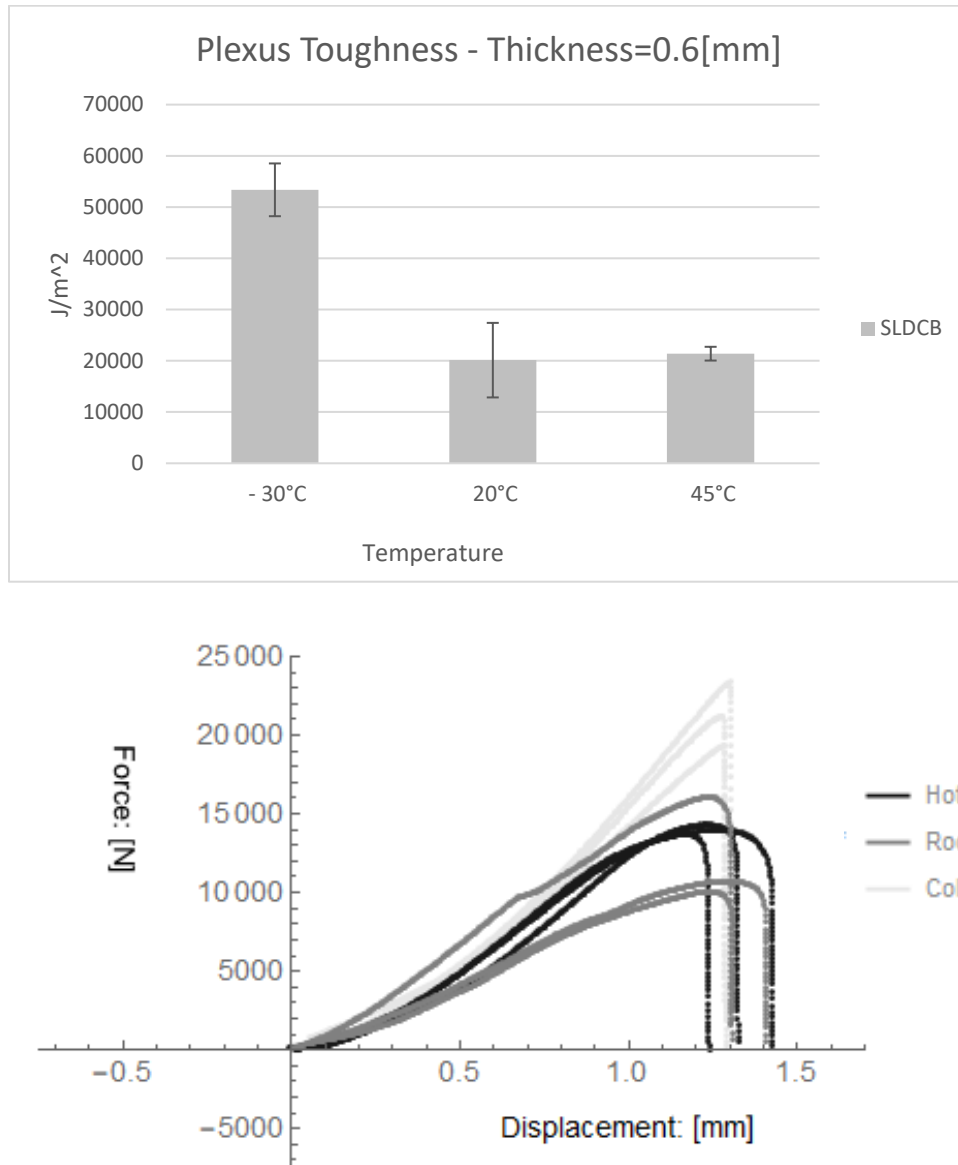


Figure 21 – SLDCB specimen results

4.1 Phase I - Pliogrip

In Figure 22, the results for the dog bone tensile specimen for Mode I strength bonded with Pliogrip can be seen.

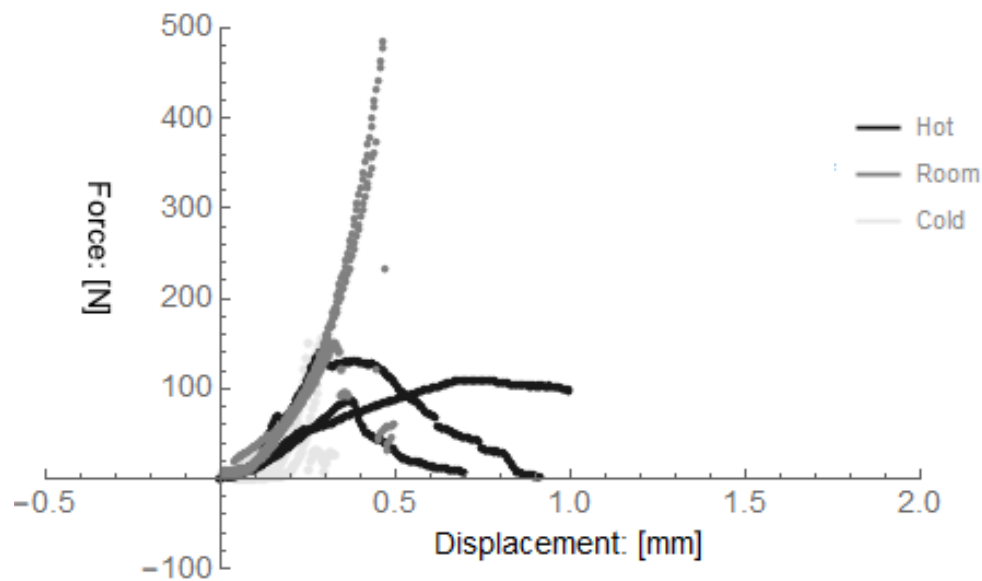
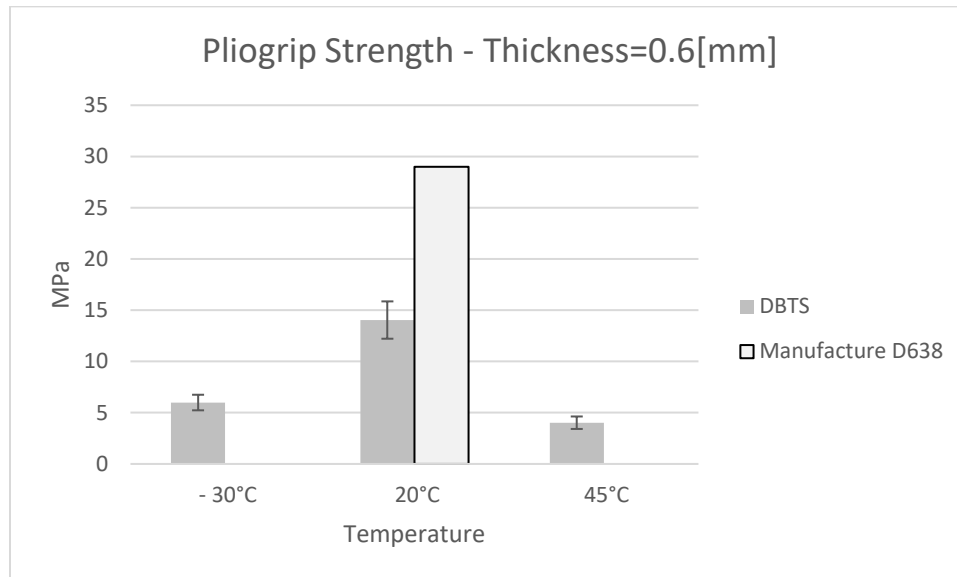


Figure 22 – DBTS specimen results

In Figure 23, the results for the dual cantilever beam specimen for Mode I toughness bonded with Pliogrip can be seen.

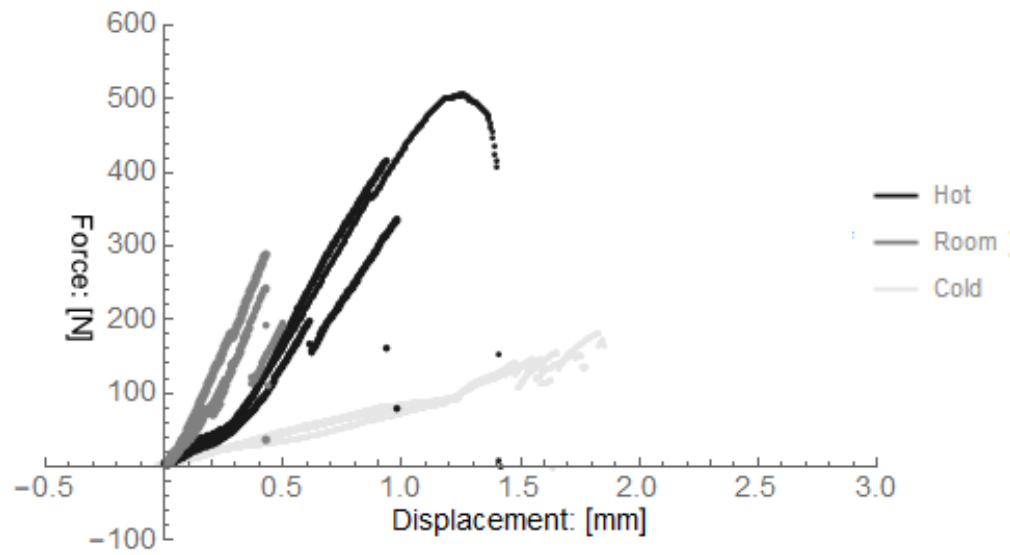
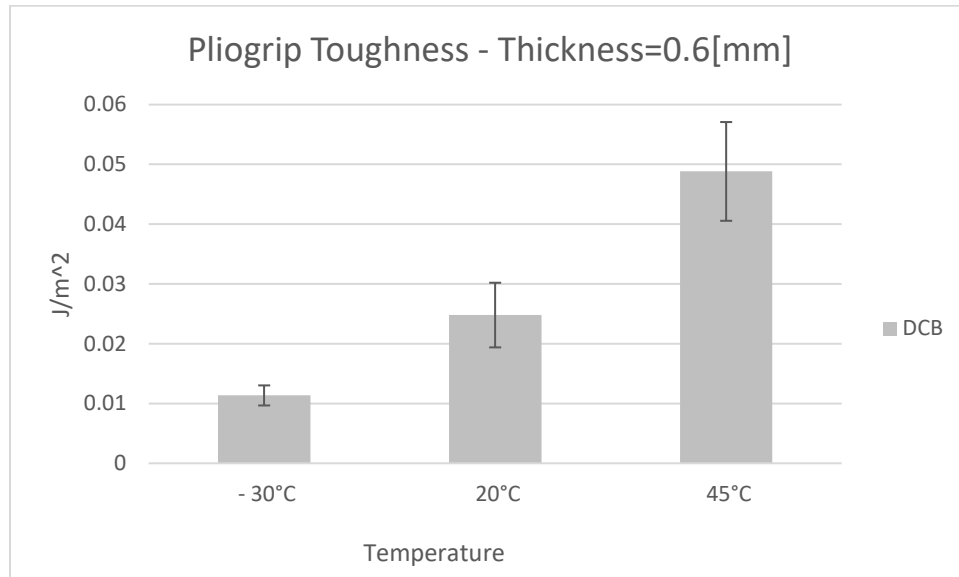


Figure 23 – DCB specimen results

In Figure 24, the results for the double lap shear specimen for Mode II strength bonded with Pliogrip can be seen.

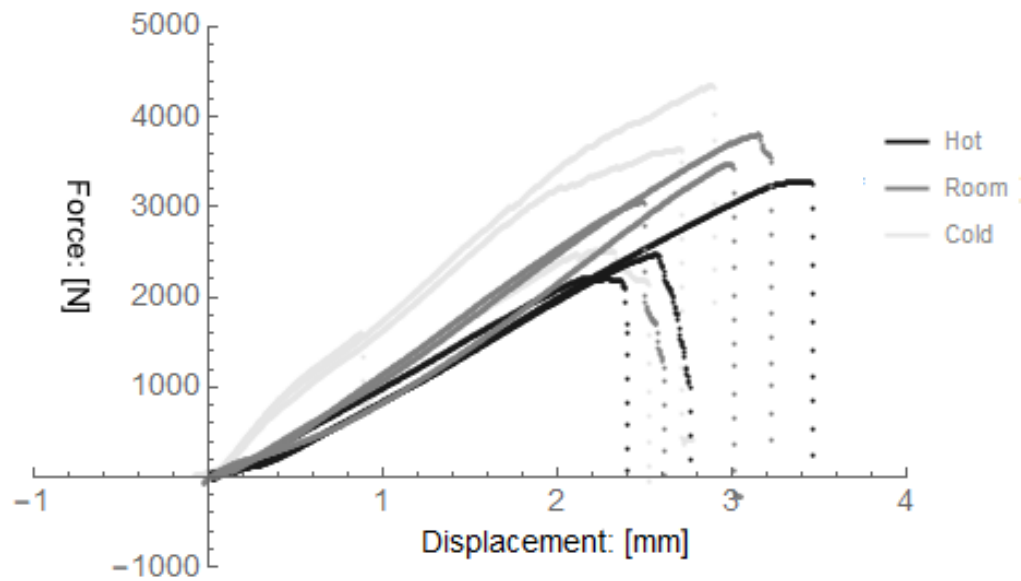
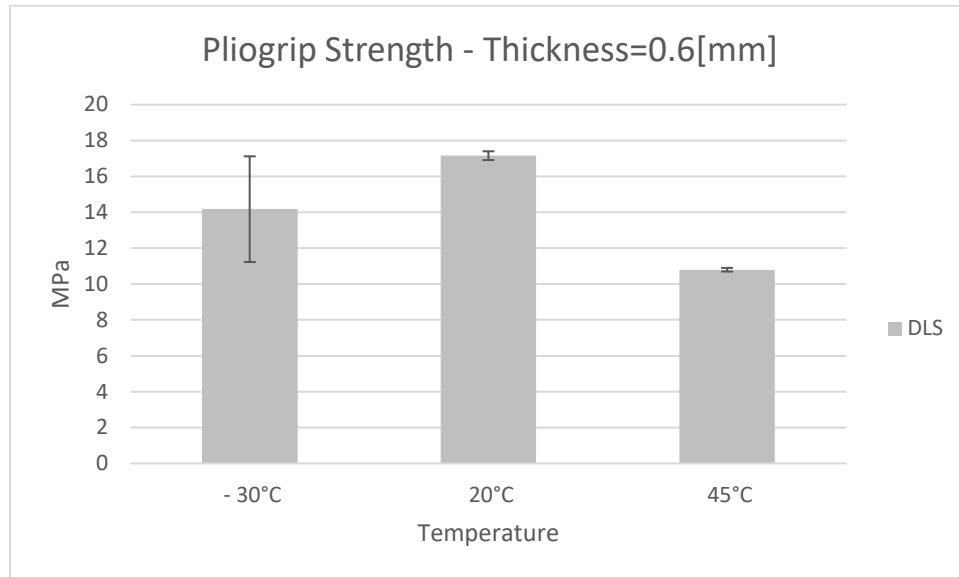


Figure 24 – DLS specimen results

In Figure 25, the results for the shear loaded dual cantilever beam specimen for Mode II toughness bonded with Pliogrip can be seen.

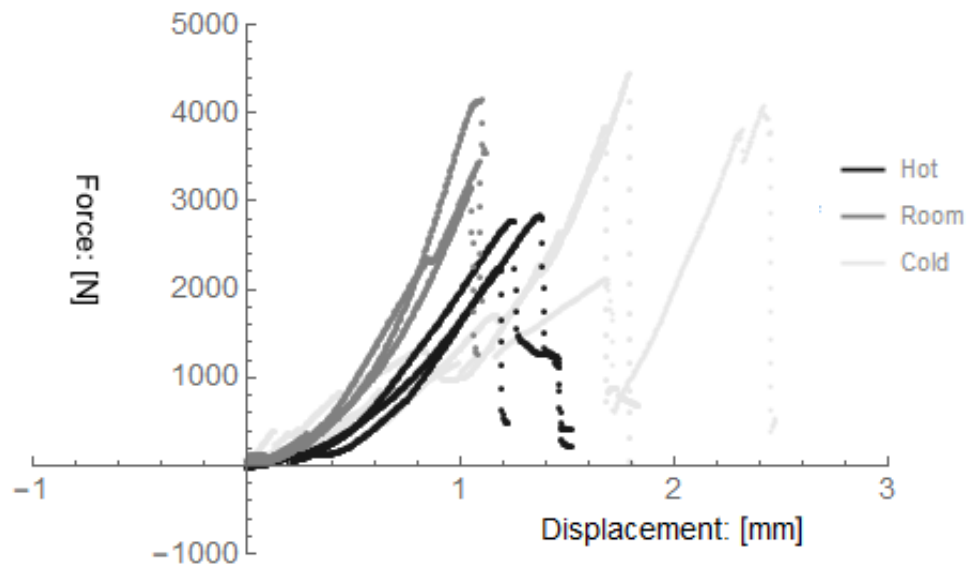
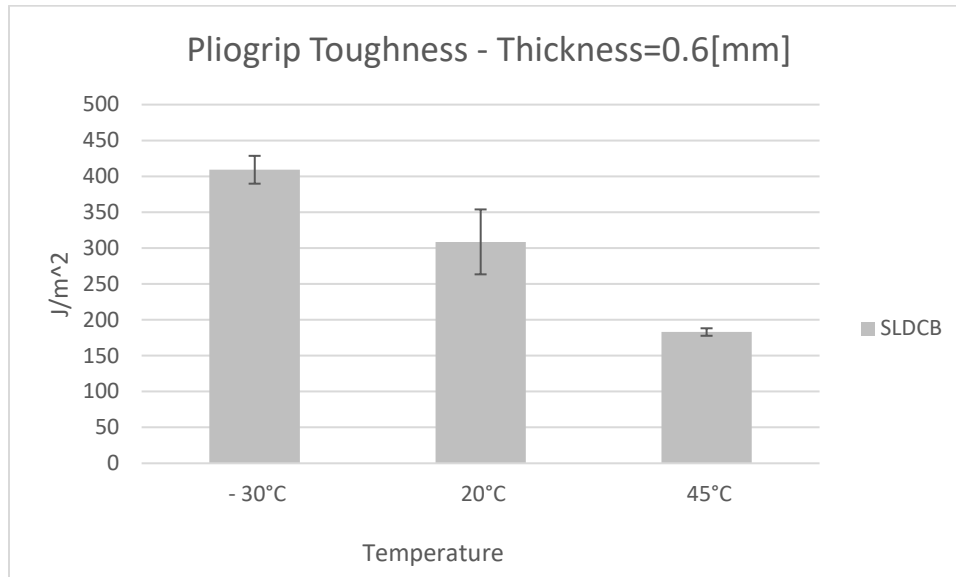


Figure 25 – SLDCB specimen results

Phase II – Plexus

Mode I

In Figure 26, the results for the dual cantilever beam for Mode I toughness bonded with Plexus with a thin bond length within the recommended working time can be seen.

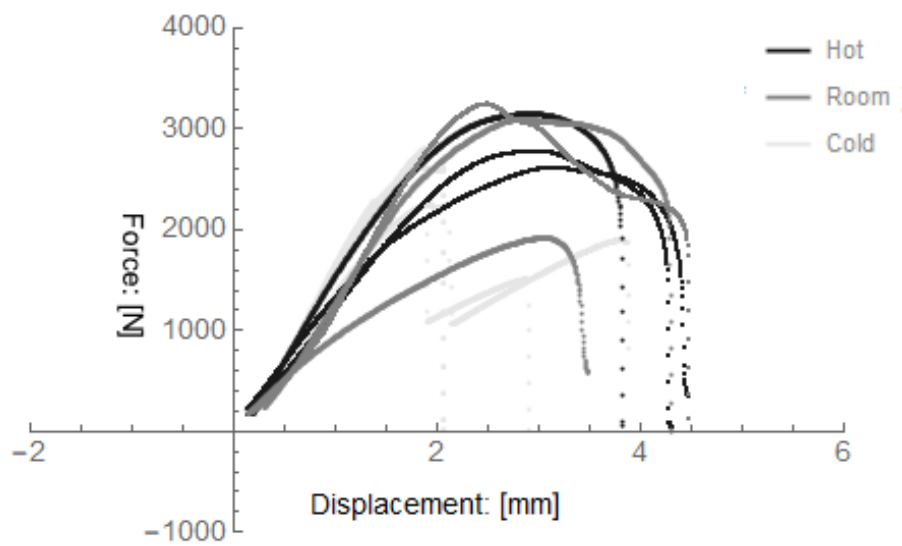


Figure 26 – DCB specimen results

In Figure 27, the results for the dual cantilever beam for Mode I toughness bonded with Plexus with a thin bond length and an expired working time can be seen.

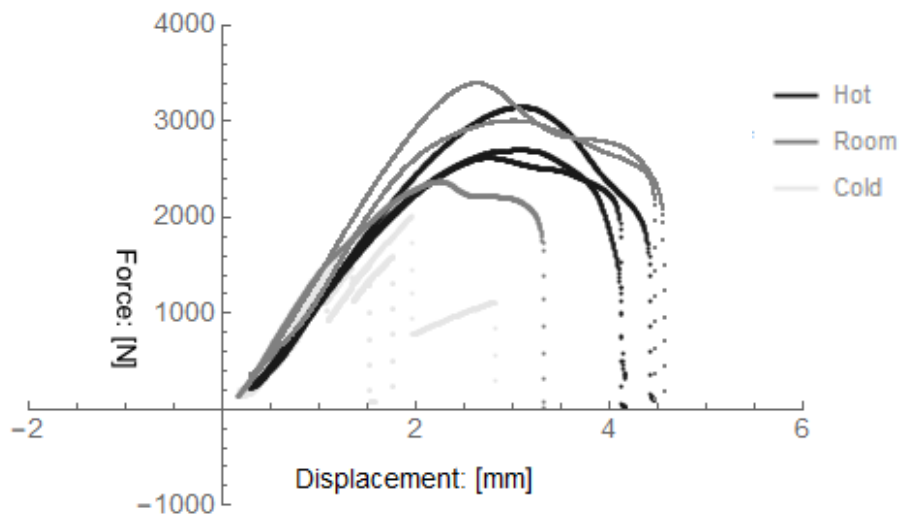
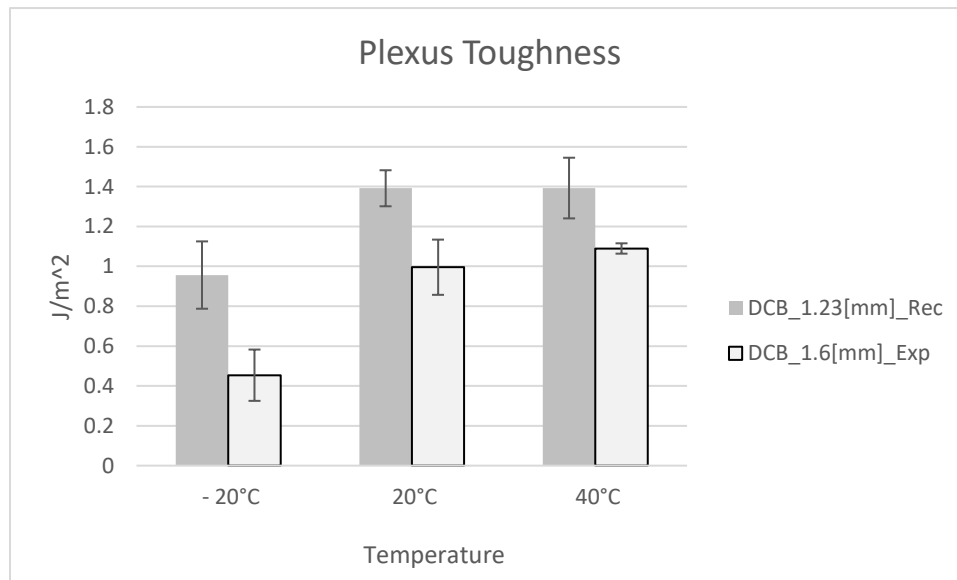


Figure 27 – DCB specimen results

In Figure 28, the results for the dual cantilever beam for Mode I toughness bonded with Plexus with a thick bond length within the recommended working time can be seen.

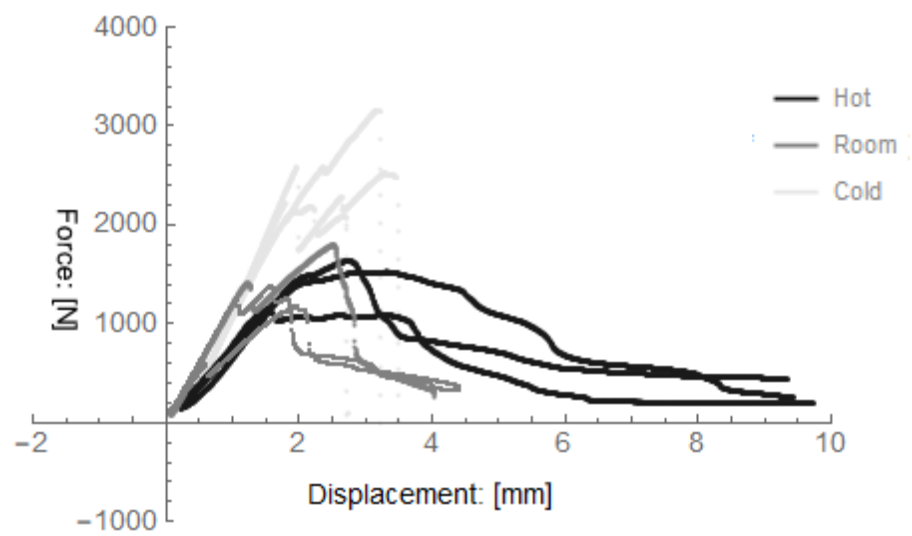


Figure 28 – DCB specimen results

In Figure 29, the results for the dual cantilever beam for Mode I toughness bonded with Plexus with a thick bond length and an expired working time can be seen.

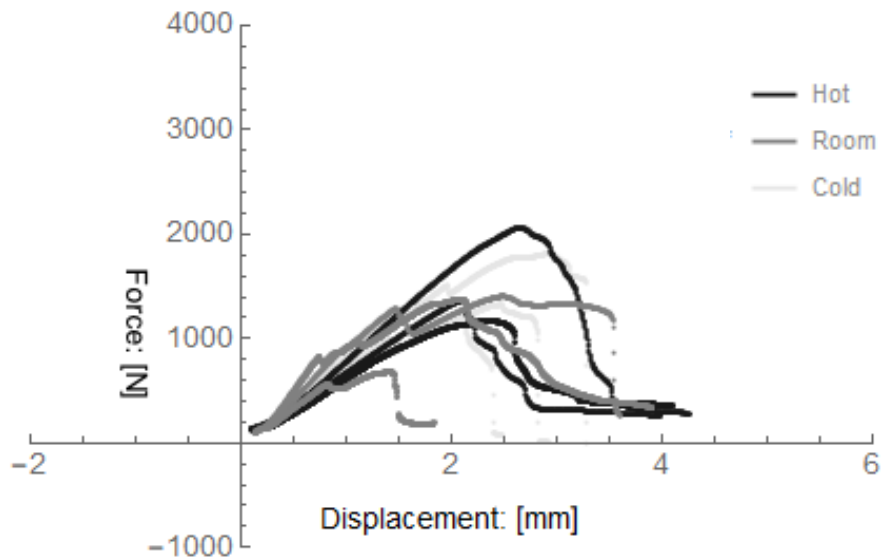
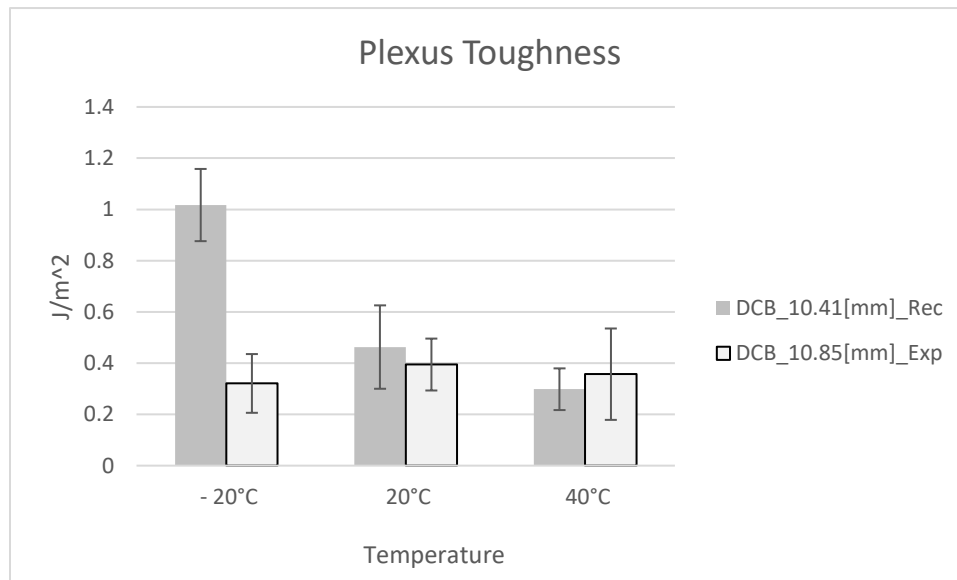


Figure 29 – DCB specimen results

Mode II

In Figure 30, the results for the shear loaded dual cantilever beam specimen for Mode II toughness bonded with Plexus with a thin bond length within the recommended working time can be seen.

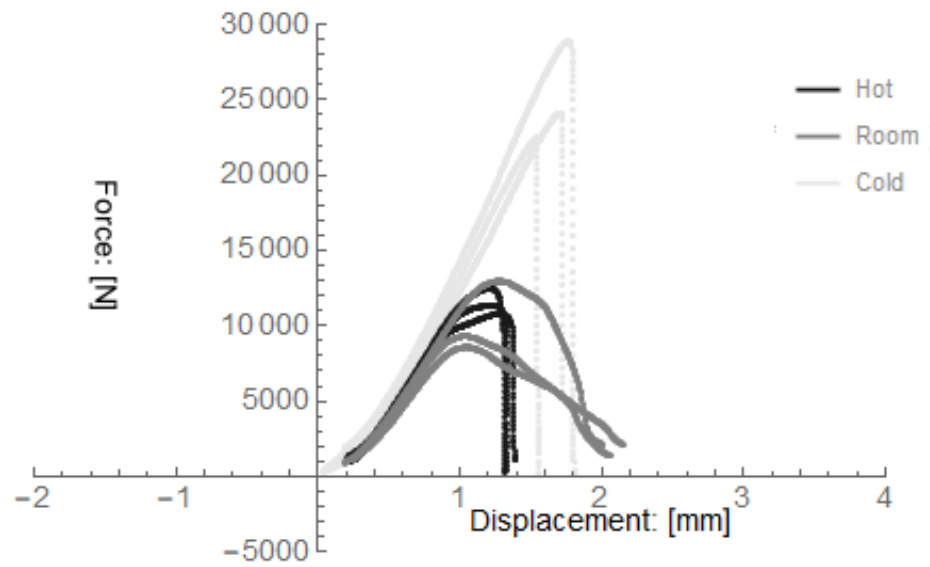


Figure 30 – SLDCB specimen results

In Figure 31, the results for the shear loaded dual cantilever beam specimen for Mode II toughness bonded with Plexus with a thin bond length and an expired working time can be seen.

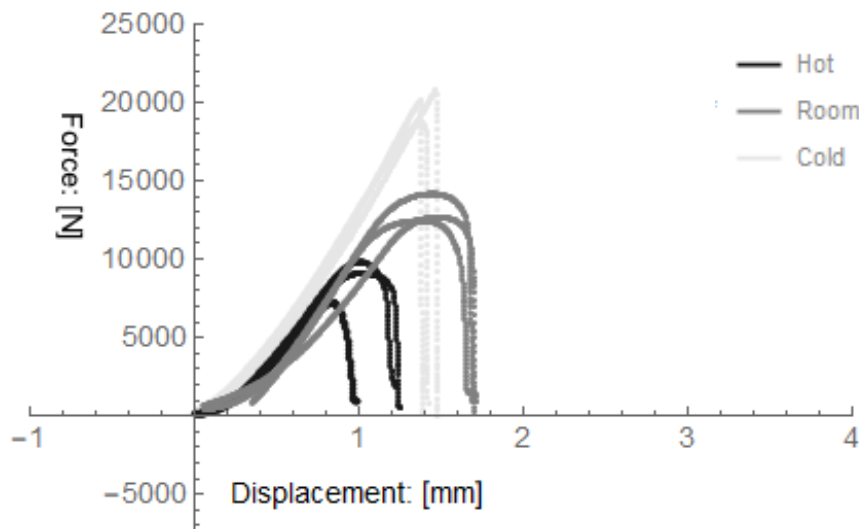
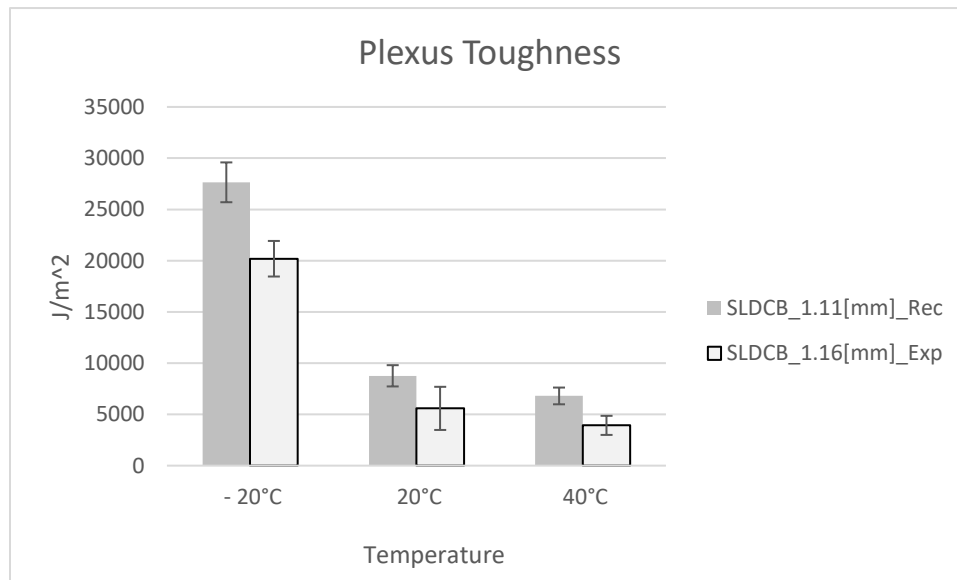


Figure 31 – SLDCB specimen results

In Figure 32, the results for the shear loaded dual cantilever beam specimen for Mode II toughness bonded with Plexus with a thick bond length within the recommended working time can be seen.

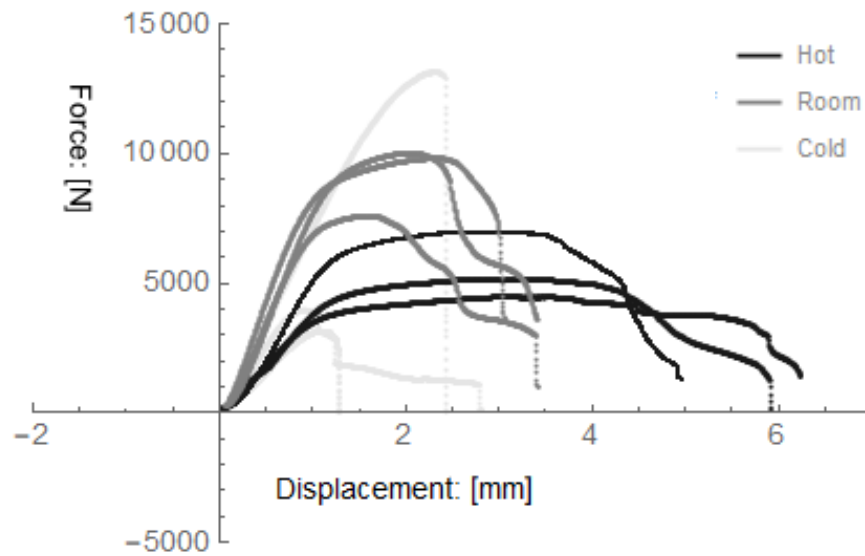


Figure 32 – SLDCB specimen results

In Figure 33, the results for the shear loaded dual cantilever beam specimen for Mode II toughness bonded with Plexus with a thick bond length and an expired working time can be seen.

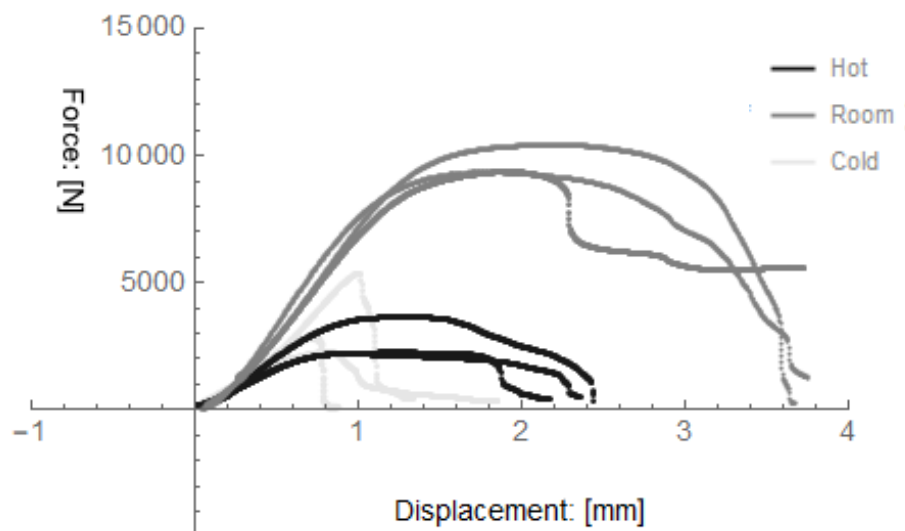
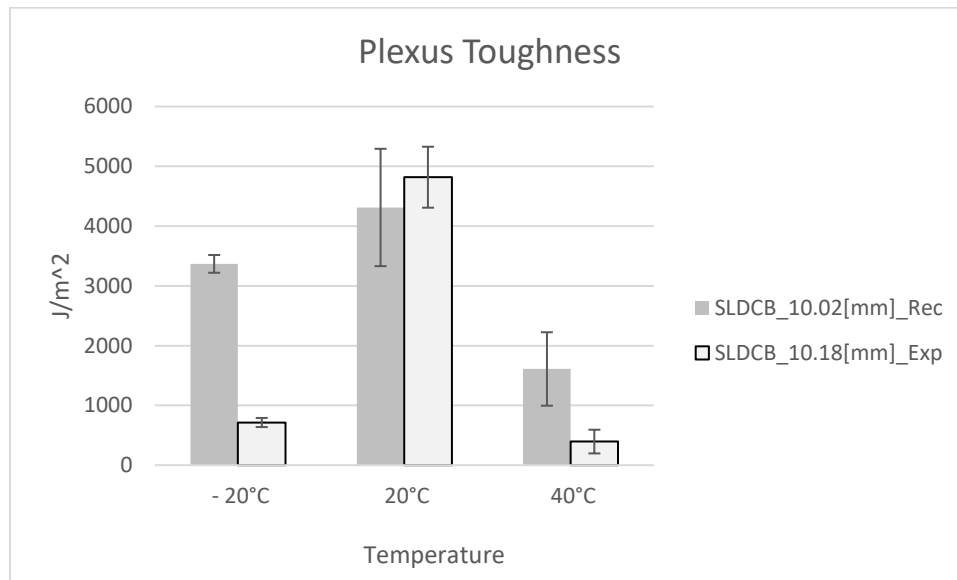


Figure 33 – SLDCB specimen results

4.2 Tabled Results – Phase I and Phase II

The average results for the three specimens and their standard deviation is reported in tables for phase I and phase II. In phase I, tables 1 and 2 are for Plexus MA832 and Pliogrip 7779/220, respectively. In phase II, table 3 is for Plexus MA832. The tables include the cohesive strength (σ) [MPa], cohesive toughness Γ [J/m²], Data provided by the manufacturer, and displacement at failure [mm], where applicable. The tables contain the variation of each temperature, bond thickness, and working time from the respective loading modes and conditions tested.

In table 4 and table 5 the statistical differences between the specimens is presented for Phase I and Phase II, respectively. The statistical differences presented uses a pooled variance t-test at a confidence level of 95%. A plus sign indicates there is a positive influence, a minus sign indicates there is a negative influence, and a blank space indicates there is not a statistical difference at the confidence level used. The warm and cold specimens are compared to the room temperature specimens. The thickness in phase II is compared between thin and thick bonds for each temperature tested. The working time in phase II is compared between recommended and expired working time for each temperature tested.

Tabled Results – Phase I

Table 1 - Results for Plexus MA832

Plexus MA832	-30°C	20°C	45°C
DBTS. σ Fig. 18	Mode I		
Cohesive strength [MPa]	16.02 \pm 2.98	12.87 \pm 4.16	7.78 \pm 0.60
Displacement [mm]	0.503 \pm 0.080	0.19 \pm 0.018	0.52 \pm 0.016
Manufacturer's data [MPa] ASTM D638 [1,12]		18.6 – 20.7	
DCB. Γ Fig. 19	Mode I		
Cohesive toughness [J/m ²]	0.483 \pm 0.058	0.664 \pm 0.109	0.575 \pm 0.068
Displacement [mm]	3.17 \pm 0.278	2.44 \pm 0.511	3.52 \pm 0.188
DLS. σ Fig. 20	Mode II		
Cohesive strength [MPa]	32.83 \pm 7.04	20.66 \pm 4.34	21.73 \pm 6.00
Displacement [mm]	7.86 \pm 4.349	3.53 \pm 0.368	3.46 \pm 0.186
Manufacture – [MPa] ASTM D1002 [52,12]		13.8-19.3	
SLDCB. Γ Fig. 21	Mode II		
Cohesive toughness [J/m ²]	53369.19 \pm 11031.3	20127.34 \pm 7274.9	21392.79 \pm 1343.6
Displacement [mm]	1.28 \pm 0.008	1.34 \pm 0.040	1.32 \pm 0.074

Tabled Results – Phase I

Table 2 - Results for Pliogrip 7779/220

Pliogrip 7779/220	-30°C	20°C	45°C
DBTS σ Fig. 22	Mode I		
Cohesive strength [MPa]	5.99 \pm 0.759	14.04 \pm 1.822	4.02 \pm 0.608
Displacement [mm]	0.28 \pm 0.024	0.49 \pm 0.008	0.86 \pm 0.124
Manufacture σ [MPa] ASTM D638 [1,13]		29	
DCB Γ Fig. 23	Mode II		
Cohesive toughness [J/m ²]	0.011 \pm 0.005	0.024 \pm 0.005	0.048 \pm 0.012
Displacement [mm]	1.75 \pm 0.098	0.423 \pm 0.028	1.11 \pm 0.201
DLS σ Fig. 24	Mode II		
Cohesive strength [MPa]	14.17 \pm 2.94	17.15 \pm 0.244	10.79 \pm 0.102
Displacement [mm]	2.72 \pm 0.156	2.93 \pm 0.249	2.87 \pm 0.419
SLDCB Γ Fig. 25	Mode II		
Cohesive toughness [J/m ²]	409.2 \pm 121.21	308.62 \pm 45.23	182.97 \pm 5.22
Displacement [mm]	1.97 \pm 0.318	1.11 \pm 0.029	1.40 \pm 0.141

Tabled Results – Phase II

Table 3 - Results for Plexus MA832 variation in thickness, working time and temperature

Plexus MA832		-20°C	20°C	40°C
Thickness	Working time	Mode I – DCB - Cohesive toughness [J/m ²]		
1.23 [mm]	Rec. Fig. 26	0.956 ±0.168	1.39 ±0.090	1.39 ±0.152
Displacement	[mm]	2.93 ±0.694	4.10 ±0.432	4.18 ±0.289
1.60 [mm]	Exp. Fig. 27	0.453 ±0.128	0.995 ±0.474	1.08 ±0.025
Displacement	[mm]	2.02 ±0.529	4.11 ±0.537	4.24 ±0.168
10.41 [mm]	Rec. Fig. 28	1.01 ±0.307	0.462 ±0.162	0.298 ±0.081
Displacement	[mm]	3.10 ±0.374	4.30 ±0.216	9.53 ±0.124
10.85 [mm]	Exp. Fig. 29	0.320 ±0.114	0.394 ±0.101	0.356 ±0.178
Displacement	[mm]	2.86 ±0.329	3.11 ±0.941	3.96 ±0.256
		Mode II- SLDCB - Cohesive toughness [J/m ²]		
1.08 [mm]	Rec. Fig. 30	32567.50 ±7139.81	8764.39 ±1037.75	6800.90 ±817.92
Displacement	[mm]	1.72 ±0.101	2.09 ±0.081	1.35 ±0.040
1.16 [mm]	Exp. Fig. 31	20188.22 ±1735.31	5585.27 ±2105.54	3928.17 ±931.03
Displacement	[mm]	1.45 ±0.040	1.74 ±0.032	1.15 ±0.108
9.86 [mm]	Rec. Fig. 32	3368.23 ±3847.09	4311.56 ±981.36	1609.92 ±614.21
Displacement	[mm]	2.19 ±0.643	3.33 ±0.169	5.66 ±0.498
10.18 [mm]	Exp. Fig. 33	714.53 ±534.68	4817.76 ±509.95	395.57 ±198.15
Displacement	[mm]	1.37 ±0.387	3.69 ±0.069	2.32 ±0.097

*Rec.=Recommended, Exp.= Expired

Tabled Results – Phase I

Table 4 – Summary of Statistical Differences Phase I

	Temperature		
	-30°C	45°C	20°C – <i>Ref.</i>
Pliogrip 7779/220			
DBTS	-	-	
DCB	-	+	
DLS	-	-	
SLDCB		-	
Plexus MA832			
DBTS		-	
DCB	-		
DLS	+		
SLDCB	+		

*Ref.=Reference Temperature

Tabled Results – Phase II

Table 5 – Summary of Statistical Differences Phase II

Plexus MA832	Thickness	Working Time	Temperature		
			-20°C	20°C	40°C
Mode I					
DCB	Thin	Rec.	-	<i>Ref.</i>	
DCB	Thin	Exp.	-	<i>Ref.</i>	
Rec. to Exp.			-		-
DCB	Thick	Rec.	+	<i>Ref.</i>	
Thin to Thick				-	-
DCB	Thick	Exp.		<i>Ref.</i>	
Rec. to Exp.			-		
Thin to Thick				-	-
Mode II					
SLDCB	Thin	Rec.	+	<i>Ref.</i>	-
SLDCB	Thin	Exp.	+	<i>Ref.</i>	
Rec. to Exp.			-	-	-
SLDCB	Thick	Rec.		<i>Ref.</i>	-
Thin to Thick			-	-	-
SLDCB	Thick	Exp.	-	<i>Ref.</i>	-
Rec. to Exp.					-
Thin to Thick			-		-

*Ref.=Reference Temperature, Rec.=Recommended, Exp.=Expired

5. Discussion

Specific to adhesives are some failure types that apply to the interaction between the adherents, or materials the adhesive layer is joining, and the adhesive. Namely, there are three main failure types for adhesives; adhesive, cohesive, and substrate. The failure types can be seen in Figure 34. The first, seen on the left, is cohesive failure where the crack that forms in the joint lies completely between the adhesive layer. This failure type is reflective of the true adhesive behavior. The second, seen in the middle, is adhesive failure where the crack that forms in the joint lies between the adhesive and substrate (adherent) region. This failure type is reflective of the adhesive and substrate interaction. The last type, seen on the right, is substrate failure, where the substrate material has less strength than the adhesive, and the crack that forms is completely in the substrate region. This last type of failure gives little insight into the behavior of the adhesive, and often indicates an adhesive with less strength would produce a joint with similar loading capabilities. In testing, the failure types the joint sees can often be mixed. The failure type in this type of case is attributed to which type is most dominant. For example, in the right substrate failure case presented, there are regions of both adhesive, and cohesive failure, but the majority of the failure is within the substrate, leaving the failure type to be substrate. The failure types desired for adhesive studies are cohesive, or adhesive when an interfacial interaction is desired.



Figure 34 – Adhesive Failure type: Left-Cohesive, Middle-Adhesive, Right-Substrate

The tests in general were consistent within each specimen type, under the exposed conditions for the adhesive failure. Indicating that the specimens failed in similar manners. The Plexus specimen's main adhesive failure mode was cohesive. These results suggest that the specimens represent the adhesives true behavior as failure occurred between the adhesive layer. The Pliogrip specimen's main adhesive failure mode was mixed between substrate and cohesive. These results suggest that the specimens represent an interaction between the adhesive and the substrate material. In discussion with the manufacturer, for the substrate used, this result was to be expected [13].

The Plexus specimens in Phase I and II during cold temperature testing often displayed a brittle like material behavior, where there is a sharp transition from the

elastic region to failure. Worth noting, in Plexus testing, is one of the DLS specimens during cold temperature testing slipped in the loading grips, as its displacement was about three times the displacement of the previous two tests. Another specimen worth discussion is one of the SLDCB specimens with a thick bond carried over two times the load than the previous two specimens. Upon inspection of the bond region after the test there was no noticeable difference in failure type compared to the other specimens. It is worth noting that, another study has found increased variability in thick adhesive bonds [6] and the increased load carry ability of this one specimen is likely an outlier. The room and warm temperature testing for Plexus showed similar loading curves with the warm temperature specimens tending to have less strength. The warm temperature specimens also tended to not fail abruptly and continue to carry a reduced load until failure.

The Pliogrip specimens bonded with SMC typically had a sharp transition from the elastic region to failure. This transition is attributed to the substrate material, and nature of Pliogrip to peel with the material used. In mode I loading, a few of the warm temperature specimens did have some toughness, where the transition from the elastic region to failure had some continued loading capability. Worth noting in the Pliogrip cold temperature testing, is one of the SLDCB specimens had a shift in the support block of the fixture, which can be seen at 1.7 [mm] displacement, the specimens was allowed to continue to load, and behaved similarly to the previous two specimens but at an extended displacement.

The chamber could heat the specimens to 45°C in approximately 30 [minutes]. The relative humidity during the warm test remained between 13 and 15 %

for both the front and rear sensors. The chamber could cool the specimen to -30°C in approximately 55 minutes. The cooling procedure had two steps to reach this temperature. The first step was to cool the chamber and specimen to -15°C ; this could be done in approximately 30 minutes. At this temperature, the chamber seal would need to be broken for the addition of a perforated container of dry ice that would slot in above the fan assembly and add additional cooling power to the chamber. Upon resealing the chamber with the dry ice the specimen would reach the required -30°C in an additional 25 minutes. It is worth noting that the cooling rate declined after the first test, and additional testing took longer to reach required temperatures.

The relative humidity during the cold temperature testing varied during the testing. The variation is contributed to the humidity added by the dry ice and the opening of the door mid-cooling for the perforated tray. The relative humidity gradually dropped during the cold temperature testing. The front sensor went from 100 to 90 % relative humidity and the rear from 85 to 75%. The increase from rear sensor to front sensor is attributed with more direct contact with the dry ice and fan assembly, and the opening of the chamber door. Overcooling of the specimen from the dry ice was not a concern. The heating and cooling circulator maintains the temperature for the chamber at the desired setting, so despite the sublimation temperature of -78°C for the dry ice, the chamber would hold -30°C . The tradeoff is at this point the circulator would add heat to the chamber to maintain -30°C .

6. Conclusion

The effect of temperature, thickness, and working time on adhesive behavior was studied for the body of work above. The adhesive behavior was observed with specimens that ideally represent the cohesive strength and toughness for mode I and mode II loading cases. These properties are what is needed to successfully use a cohesive zone model [2,6,28,29,40]. For mode I cohesive strength, the Dog Bone Tensile Specimen (DBTS) was used to load the adhesive in tension. The mode I cohesive toughness was found using the Dual Cantilever Beam (DCB) specimen which also loads the adhesive in tension [40,41]. For mode II cohesive strength, the Double Lap Shear (DLS) test, found in ASTM D3528, is used to load the adhesive in a shear state [42]. The mode II cohesive toughness was found using the Shear Loaded Dual Cantilever Beam (SLDCB) specimen to also load the adhesive in shear [29,44]. The adhesives used in the study are Plexus MA832, a two-part methacrylate structural adhesive, and Pliogrip 7770/220b, a two-part urethane structural adhesive. The temperatures tested were -30°C, -20°C, 20°C, 40°C, and 45°C. These temperatures are similar to the range that structural products must provide load carrying ability in normal use in North America and throughout the world. The relative humidity during temperature testing; at cold temperature was on average 84%, at room temperature was 30%, and at warm hot temperatures 14%. The thickness tested in phase I was 0.6 [mm], and in phase II for the thin bond was 1.27 [mm] and for the thick bond was 10.38 [mm]. The working time had a control group that was bonded within the recommended manufacture time, and an expired working time group that was not bonded until 10 [min] had passed from the recommended time.

The results from experimental testing indicate that the adhesives tested are negatively influenced by adverse temperature conditions. An exception is seen with Plexus where the DLS and SLDCB specimens with thin bonds during cold temperature testing had a positive influence from the adverse temperature. This behavior is also found in Kang's DLS joints specimens where its highest joint strength occurred at cold temperatures [2]. Another exception to this is seen with Pliogrip, where the DCB specimens during warm temperature testing had a positive influence from the adverse temperature. It is worth noting that, the testing temperature was not near the glass transition temperature of either adhesive, which is known to degrade adhesive behavior [34]. The results from Phase II testing show that increasing the bond thickness overall has a negative influence on adhesive behavior for both loading modes across the temperatures tested. The results from Phase II testing also show that bonding past the recommended working time can have a negative influence on adhesive behavior for both loading modes. However, it is worth noting that, some load carrying ability was still found with expired working times. Indicating that the recommended working time is not an ultimatum that upon surpassing leads to catastrophic failure. It is still not recommended to design with this bonding procedure.

In conclusion, this study finds that adhesive performance for Plexus MA832 and Pliogrip 7779/220b can be affected negatively in response to adverse temperature regimes, and the former to increasing thickness of bond, and expired working times. This response is recommended to be applied during the design of an adhesive joints that will provide service with these adhesives under the conditions tested.

Future Work and Recommendations

In future work the results can be implemented into finite element analysis packages that use cohesive zone modeling to help aide the design of adhesive joints in modeling space. To extend the modeling capability to incorporate other materials and adhesives, additional testing would be required to give the same confidence the current results provide for the parameters varied. A linear regression could be used from the results to provide properties at in-between temperatures. For variation of other temperatures and parameters that may affect adhesive behavior it is recommended that confirmation of the analysis be conducted with experimental testing before implementation into service.

Future testing of interest, to the author, would be the effect of cyclic temperature loading on adhesives, and the long-term effect of changing humidity seen through the ambient outdoor environment on corrosion in bond lines. An experimental set-up of interest would be the testing a “racking” load. Where the adhesive would lie between two plates, with the bottom plate static, and the top plate pulled from the corner perpendicularly from the edge. This racking load would create a mixed peeling load on the adhesive. This scenario could also be tied to a finite element analysis that would be able to provide confidence to 3-D interactions of traction separation laws.

A recommendation in the manufacturing of test specimens for adhesive study is to control bond lengths with the use of positive surfaces over applying PTFE tape. As application of the tape is rather tedious.

Bibliography

- [1] A.S. D638, Standard Test Method for Tensile Properties of Plastics, West Conshokecken, PA: ASTM International, 2014.
- [2] Kang S , Kim M, “Evaluation of cryogenic performance of adhesives using composite-aluminum double-lap joints,” *Composite Structures* 78, vol. 2007, pp. 440-446, 2007
- [3] Kendall, Kevin, “Adhesion: Molecules and mechanics” *Science* 263, no 5154 (1994); 1720
- [4] Shah, & Tarfaoui. (2016), “Effect of adhesive thickness on the Mode I and II strain energy release rates, Comparative study between different approaches for the calculation of Mode I & II SERR’s” *Composites Part B*. 96, 354-363.
- [5] Xuan C, Yulong L, “An experimental Technique on the Dynamic Strength of Adhesively Bonded Single Lap Joints,” *Journal of Adhesion Science & Technology*, February 2010:24(2):291-304. Academic Search Premier, Ipswich, MA. Accessed July 16, 2017
- [6] Marzi, Biel, & Stigh., “On experimental methods to investigate the effect of layer thickness on the fracture behavior of adhesively bonded joints,” *International Journal of Adhesion and Adhesives*, Vol. 31, issue 8, pp. 840-850, 2011.
- [7] Messler and W. Savage, "Joining of Advanced Materials," Burlington: Elsevier Science, 2013.
- [8] Daimler Trucks North America, "Quick Facts," Daimler, 2015. [Online]. Available: <http://www.daimler---trucksnorthamerica.com/inside/quick---facts.aspx>. [Accessed 10 June 2016].
- [9] Nicholson, C. et al, “History of Adhesives”, BSA Educational Services Committee, vol. 2.2, 1991
- [10] Sauter F, “Studies in organic archaeometry I: identification of the prehistoric adhesive used by the “Tryolean Iceman” to fix his weapons,” *ARKAT, USA*, vol. 5, pp. 735-747,2000
- [11] Pike, R, “Adhesive,” *encyclopedia Britannica*, 15 September 2017. [online]. Available: <https://www.britannica.com/technology/adhesive> [Accessed 05 July 2017]
- [12] ITW Plexus, "Plexus MA832," March 2003. [Online]. Available: <http://www.itwplexus.co.uk/images/uploads/tds/832.pdf>. [Accessed 16 March 2016].

- [13] Ashland Inc., <http://www.itwplexus.co.uk/images/uploads/tds/832.pdf>, 28 May 2009. [Online]. Available: [http://www.ashland.com/Ashland/Static/Documents/APM/PLIOGRIP%207770%20\(7400%20%207654\)%202437%20v2%20EN-1%20F2\[1\].pdf](http://www.ashland.com/Ashland/Static/Documents/APM/PLIOGRIP%207770%20(7400%20%207654)%202437%20v2%20EN-1%20F2[1].pdf). [Accessed 16 March 2016].
- [14] Inglis, C.E., "Stresses in a plate due to the presence of cracks and sharp corners," *Trans. Inst. Nav. Archit. London* 55, 1913, pp.210-230
- [15] Griffith, A.A., "Phenomena of rupture and flow in solids," *Philos. Trans. R. Soc, London Ser. A*221, 1920, pp. 163-198
- [16] Irwin, G.R., "Fracture dynamics," *Trans. Am. Soc. Met.* 40A, 1948, pp. 147-166
- [17] Orowan, E., "Fracture and strength of solids," *Rep Prog Phys*, vol. 12, 1949, pp.185-232
- [18] Irwin, G.R., "Analysis of stresses and strains near the end of a crack traversing in a plate," *Journal of applied mechanics*, vol. 24, 1957, pp.361-364
- [19] Irwin, G.R., "Onset of fast crack propagation in high strength steel and aluminum alloys," *Proceedings of the second Sagamore ordnance materials conference*, vol. 2, 1956, pp.289-305
- [20] Irwin, G.R., Kies, J.A., "Critical energy rate analysis for fracture strength," *Weld Journal Res Suppl*, vol. 19, 1954, pp.193-198
- [21] Irwin G.R., "Fracture testing of high-strength sheet materials under conditions appropriate for stress analysis," Report 5486, Naval Research Laboratory, July 27, 1960
- [22] Wells, A.A., "Application of fracture mechanics at and beyond general yielding," *Br Weld Journal*, vol. 10, 1963, pp.663-570
- [23] Rice, J.R., "A path independent integral and the approximate analysis of strain concentration by notches and crack," *Journal of Applied Mechanics*, vol. 35, 1968, pp. 379-386
- [24] Hutchinson, J.W., "Singular behavior at the end of a tensile crack in a hardening material," *Journal of mechanics and physical solids*, vol. 16, 1968, pp. 13-31
- [25] Shih, C.F., German, M.D. "Requirements for a one parameter characterization of crack tip fields by the HRR singularity," *International Journal of fracture*, vol.17, 1981, pp.27-43

- [26] Barenblatt, G. I., "The mathematical theory of equilibrium cracks in brittle fracture," *Advances in Applied Mechanics*, vol. 7, 1962, pp.55-129
- [27] Dugdale, D.S., "Yielding of steel sheets containing slits," *Journal of Mechanics, Physics, and Solids*, vol. 8, 1960, pp.100-104
- [28] M.D.Banea, "Mode I fracture toughness of adhesively bonded joints as a function of temperature: Experimental and numerical study," *International Journal of Adhesion and Adhesives*, vol. 31 issue 5, July 2011, pp 273-279
- [29] J. G. Hortnagl, "Determination of Cohesive Parameters for Aerospace Adhesives," Corvallis, 2013.
- [30] M. Alam, B. Grimm, J.P. Parmigiani, "Effect of incident angle on crack propagation at interfaces" *Engineering Fracture Mechanics*, vol. 162, pp. 155-163, 2016.
- [31] M. D. Thouless, J. P. Parmigiani, "The Effects of Cohesive Strength and Toughness on Mixed---Mode Delamination of Beam-Like Geometries," *Engineering Fracture Mechanics*, vol. 74, no. 17, pp. 2675-2699, 2007.
- [32] I.S.A.C. Karl-Heinz Schwalbe, "The SIAM method for applying cohesive models to the damage behavior of engineering materials and structures," *GKSS*, no1. 1-78, 2009
- [33] T. K. J. Bent F. Sorensen, "Determination of Cohesive Laws by the J Integral Approach," *Engineering Fracture Mechanics*, vol. 70, no. 14, pp. 1841----1858, 2003
- [34] Carbas, R. J. C., et al. "Effect of Cure Temperature on the Glass Transition Temperature and Mechanical Properties of Epoxy Adhesives." *The Journal of Adhesion*, vol. 90, no. 1, 2014, pp. 104–119.
- [35] Ahmad, Z., et al. "Epoxy Adhesives Modified With Nano- and Microparticles for In Situ Timber Bonding: Effect of Environment on Mechanical Properties and Moisture Uptake." *Journal Of Engineering Materials And Technology-Transactions Of The Asme*, vol. 132, no. 3, 2010, pp. 031016 (8).
- [36] Budhe, Rodriguez-Bellido, Renart, Mayugo, & Costa, (2014), "Influence of pre-bond moisture in the adherents on the fracture toughness of bonded joints for composite repairs," *International Journal of Adhesion and Adhesives*, 49, 80-89

- [37] Imanaka, M., Iwata, T., “Effect of adhesive layer thickness on fatigue strength of adhesively bonded butt, scarf and butterfly type butt joints.” *International Journal of Fracture*, V. 80, issue 4, 1996, pp. vR69-R76
- [38] Platt, J., “Application time and shear bond strength of one-bottle adhesive.” *Journal of dental research*, V. 79, 2000, pp. 508
- [39] El-Din, A., & Abd El-Mohsen, M. (2002). Effect of changing application times on adhesive systems bond strengths. *American Journal Of Dentistry*, 15(5), 321-324.
- [40] S. Li, “The effects of shear on delamination in layered materials,” *Journal of the mechanics and physics of solids*, vol. 52, pp. 193-214,2003.
- [41] ASTM D3433-99. 2012. Standard test method for fracture strength in cleavage of adhesives in bonded joints, West Conshohocken, PA: ASTM International, 2012.
- [42] ASTM D3528-96. 2016, Standard Test Method for Strength Properties of Double Lap Shear Adhesive Joints by Tension Loading, West Conshohocken, PA: ASTM International, 2016.
- [43] Instron testing grips , accessed: <http://www.instron.us/en-us/products/testing-accessories/grips/static-tensile-grips/mechanical-wedge-action-grips/2716-002>
- [44] H. Tada, *The Stress Analysis Cracks Handbook*, Hellertown, PA: Del Research, 1973.
- [45] www.McmasterCarr.com
- [46] Durkee J, Kuhn A, “Wettability measurements and cleanliness evaluation without substantial cost,” *Contact angle, Wettability and Adhesion*, Vol 5. Pp.115-138, 2008
- [47] Ojha M, Dalakos G, Panchamgam S, et al, “Effects of surface structure on the behavior of a heated contact line,” *Contact angle, wettability and Adhesion*, Vol. 5, pp. 3-23, 2008
- [48] J. Meraz, et al, (2016) “Temperature chamber for adhesive bonding properties from mode specific testing specimens,” *IMECE2016*, Phoenix Convention Center Phoenix, AZ, Nov. 11-17,2016, ASME
- [49] J. Meraz, “Design of a Temperature Chamber for Adhesive Testing,” Corvallis, 2015

[50] Julabo USA Inc., "FP50---HE Refrigerated/Heating Circulator," Julabo USA Inc., 2015. [Online]. Available: <http://www.julabo.com/us/products/refrigerated---circulators/refrigerated---heating---circulators/fp50---he---refrigerated---heating---circulator>. [Accessed 05 February 2016].

[51] Flex---A---Lite, "Remote Mount 7 1/2---inch Cooler with Electric Fan with AN Fittings," ColeQComm, 2015. [Online]. Available: <https://www.flex---a---lite.com/oil---fuel---coolers/coolers/remote---mount---7---1---2---inch---cooler---with---electric---fan---with---an---fittings.html>. [Accessed 15 March 2016].

[52] ASTM D1002-10, Standard Test Method for Apparent Shear Strength of Single-lap-Joint Adhesively Bonded Metal specimens by tension Loading (Metal-to-Metal), West Conshohocken, PA: ASTM International, 2010.

Appendix

A bill of materials

Quantity	Item	Index*	Description	Cost
10	Plexus MA832	n/a	380 ml -Plexus	\$47
4	Pliogrip 7779/220b	n/a	220 ml –Ashland	\$38
1	Dispensing Gun	66215A73	Plexus 10:1 mix	\$17.57
1	Dispensing Gun	7451A51	Pliogrip 1:1 mix	\$93.42
36	Mixing Nozzles	74695A84	24 PX – 12 PG	\$1.86
1	Simple Green	7428T12	1-Gallon	\$14.13
3	Isopropanol Alcohol	54845T42	473 ml	\$2.44
1	Epoxy Mold Release	n/a	398 g – Slide	\$72.74
6	6061 – 7/8”x7/8”x6’	9008K13	DCB/SLDCB	\$29.32
4	6061 – ¼”x2-1/2”x6’	8975K68	DBTS	\$27.73
2	6061 – 1/8”x6”x1’	89015K236	DLS - middle	\$17.99
4	6061 – 1/16”x6”x1’	89015K184	DLS- ends	\$10.70
1	6061- 1-1/2”x6”x1’	8975K259	Fixtures DCB	\$68.16
1	6061 – ¼” x 1’x1’	9246K13	Fixture DLS	\$45.21
1	Sand Paper	n/a	120 grit – PK50 - Grainger	\$58.12
1	Sand Paper	n/a	60 grit – PK50 - Grainger	\$56.14
2	PTFE Tape	n/a	1”x36 yds. - Grainger	\$227.09
1	Razor Blades	3962A3	PK - 100	\$7.33
74.2	Dry Ice Pellets	n/a	OSU chem store	\$1.85/ [lb.]

*- from McMaster-Carr

Raw Stock

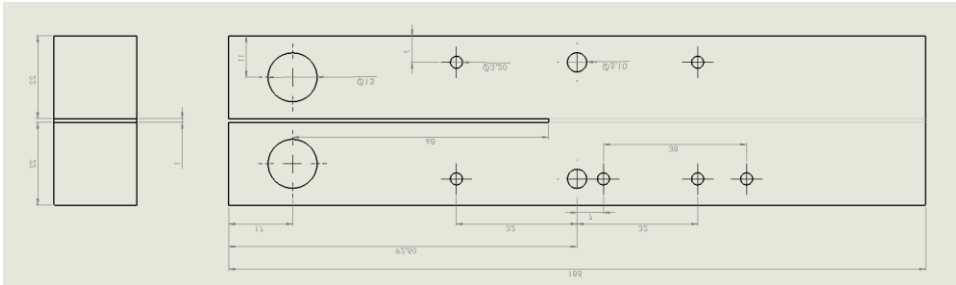
Raw stock for testing three specimens at each temperature can be seen below.



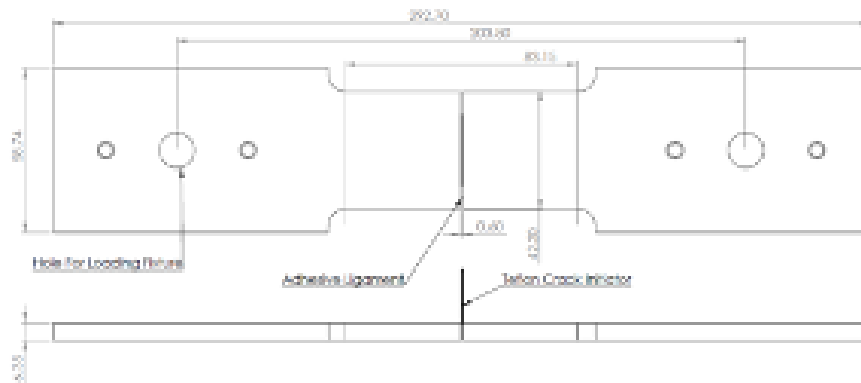
DBTS can be seen in the top left, the DCB in the top right, the SLDCB in the bottom left, and DLS in the bottom right.

Sheet drawings of specimens

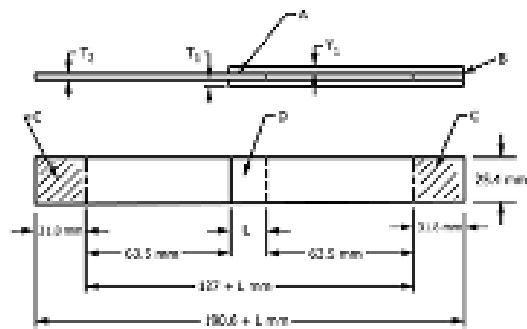
DCB



DBTS



DLS



SLDCB

